Published July 20, 2011, doi:10.4049/jimmunol.1101008

SIRPα/CD172a Regulates Eosinophil Homeostasis

Noel Verjan Garcia,* Eiji Umemoto,*,† Yasuyuki Saito,‡,1 Mikako Yamasaki,† Erina Hata,*,† Takashi Matozaki,‡,2 Masaaki Murakami,§ Yun-Jae Jung,¶ So-Youn Woo,‖ Ju-Young Seoh,‖ Myoung Ho Jang,#,** Katsuyuki Aozasa,†† and Masayuki Miyasaka*,†

Eosinophils are abundant in the lamina propria of the small intestine, but they rarely show degranulation in situ under steady-state conditions. In this study, using two novel mAbs, we found that intestinal eosinophils constitutively expressed a high level of an inhibitory receptor signal regulatory protein α (SIRPα)/CD172a and a low, but significant, level of a tetraspanin CD63, whose upregulation is closely associated with degranulation. Cross-linking SIRPα/CD172a on the surface of wild-type eosinophils significantly inhibited the release of eosinophil peroxidase induced by the calcium ionophore A23187, whereas this cross-linking effect was not observed in eosinophils isolated from mice expressing a mutated SIRPα/CD172a that lacks most of its cytoplasmic domain (SIRPα Cyto$^{-/-}$). The SIRPα Cyto$^{-/-}$ eosinophils showed reduced viability, increased CD63 expression, and increased eosinophil peroxidase release with or without A23187 stimulation in vitro. In addition, SIRPα Cyto$^{-/-}$ mice showed increased frequencies of Annexin V-binding eosinophils and free MBP^{+}CD63^{+} extracellular granules, as well as increased tissue remodeling in the small intestine under steady-state conditions. Mice deficient in CD47, which is a ligand for SIRPα/CD172a, recapitulated these phenomena. Moreover, during Th2-biased inflammation, increased eosinophil cell death and degranulation were obvious in a number of tissues, including the small intestine, in the SIRPα Cyto$^{-/-}$ mice compared with wild-type mice. Collectively, our results indicated that SIRPα/CD172a regulates eosinophil homeostasis, probably by interacting with CD47, with substantial effects on eosinophil survival. Thus, SIRPα/CD172a is a potential therapeutic target for eosinophil-associated diseases. *The Journal of Immunology*, **2011, 187: 000–000.**

The eosinophil is a multifunctional granulocyte associated with innate and Th2 immune responses against allergens and gastrointestinal helminth infections (1). Under steady-state conditions, eosinophils are particularly abundant in the small intestinal lamina propria, which they colonize prenatally in a manner dependent on CC-chemokine eotaxin-1 (2, 3) and its receptor, CCR3 (4, 5). The colonization is independent of viable commensal bacteria in the intestinal lumen (3). Eosinophils play a role in host defense against migratory helminths, particularly during secondary immune responses (6, 7). They are also involved in the development and pathogenesis of allergic diseases and gastrointestinal dysfunction through their secretion of cytotoxic proteins (8, 9).

The release of eosinophil granules, "degranulation," is an immune response common to many human diseases, including asthma (10), allergy and atopic dermatitis (11), and inflammatory bowel diseases (12, 13); little degranulation is observed under basal physiological conditions. During degranulation, activated human eosinophils release preformed cytotoxic proteins, such as major basic protein (MBP), eosinophil peroxidase (EPO), eosinophil-derived neurotoxin, and eosinophil cationic protein, as well as other cytokines, chemokines, and growth factors, from cytoplasmic granules (14). Agonists, including Igs (15, 16); cytokines, such as IFN-γ (17) and IL-6 (18); lipid mediators, such as platelet activating factor (18, 19), and the calcium ionophore A23187 (19) were shown to induce the release of eosinophil granule proteins. The stimulus-induced release of eosinophil proteins is a tightly regulated and highly selective process that occurs within minutes of agonist stimulation (14), although its regulatory mechanisms remain to be fully explored.

The survival of tissue-resident eosinophils seems to be self-regulated by tissue-specific or autocrine survival signals that the eosinophils secrete following contact with extracellular matrix proteins (20) or upon activation (16). In β common chain gene-targeted mice, which are deficient in the functional receptor for cytokines that include IL-5 and GM-CSF, eosinophils are markedly reduced in the gastrointestinal tract and peripheral blood (3). In addition, Rag-2/common γ-chain double-deficient mice were recently reported to have reduced eosinophil numbers in the

*Laboratory of Immunodynamics, World Premier International Immunology Frontier Research Center, Osaka University, Osaka 565-0871, Japan; †Laboratory of Immunodynamics, Department of Microbiology and Immunology, Osaka University Graduate School of Medicine, Osaka 565-0871, Japan; ‡Laboratory of Biosignal Sciences, Institute for Molecular and Cellular Regulation, Gunma University, Gunma 371-8512, Japan; §Laboratory of Developmental Immunology, World Premier International Immunology Frontier Research Center, Osaka University, Osaka 565-0871, Japan; ¶Department of Microbiology, Graduate School of Medicine, Gachon University of Medicine and Science, Incheon 405-835, South Korea; ‖Department of Microbiology, Graduate School of Medicine, Ewha Womans University, Seoul 120-750, Korea; #Laboratory of Gastrointestinal Immunology, World Premier International Immunology Frontier Research Center, Osaka University, Osaka 565-0871, Japan; **Division of Integrative Biosciences and Biotechnology, Pohang University of Science and Technology (World Class Universities project), Pohang 790-784, Republic of Korea; and ††Department of Pathology, Osaka University Graduate School of Medicine, Osaka 565-0871, Japan

[1]Current address: Division of Experimental Haematology, University Hospital Zurich, Zurich, Switzerland.

[2]Current address: Division of Molecular and Cellular Signaling, Department of Biochemistry and Molecular Biology, Kobe University Graduate School of Medicine, Kobe, Japan.

Received for publication April 13, 2011. Accepted for publication June 19, 2011.

M.H.J. was supported by the World Class Universities project, National Research Foundation, Ministry of Education, Science and Technology, Korea (R31-10105).

Address correspondence and reprint requests to Prof. Masayuki Miyasaka, Osaka University Graduate School of Medicine, 2-2 Yamada-oka, Suita, Osaka 565-0871, Japan. E-mail address: mmiyasak@orgctl.med.osaka-u.ac.jp

The online version of this article contains supplemental material.

Abbreviations used in this article: 7AAD, 7-aminoactinomycin D; BM, bone marrow; EPO, eosinophil peroxidase; FSC, forward light scatter; LC/MS, liquid chromatography mass spectrometry; MBP, major basic protein; PIR-B, paired Ig-like receptor B; RT, room temperature; Siglec F, sialic acid-binding Ig-like lectin F; SIRPα, signal regulatory protein α; SSC, side scatter; WT, wild-type.

intestine, but not in the lung, bone marrow (BM), or PBLs, suggesting that tissue-specific cytokine signals dependent on the common γ-chain contribute to eosinophil survival in the intestine (21).

Signaling via inhibitory receptors also seems to play a role in eosinophil homeostasis. The cross-linking of an inhibitory receptor IRp60 (CD300a) inhibits both the survival signals provided by IL-5/GM-CSF and eotaxin-dependent eosinophil migration (22). Genetic inactivation of the inhibitory paired Ig-like receptor B (PIR-B) is associated with an increased recruitment of eosinophils to the gastrointestinal tract, and PIR-B negatively regulates eotaxin-dependent eosinophil chemotaxis in vitro and in vivo (23). Given the importance of pairing activation and inhibition in the development of immune responses (24), inhibitory receptors are likely to constitute a major regulatory mechanism for counterbalancing the activating signals encountered by eosinophils to maintain tissue homeostasis.

In this study, we found that intestinal eosinophils express an inhibitory receptor signal regulatory protein α (SIRPα)/CD172a at high levels and a degranulation marker CD63 at low, but significant, levels and that SIRPα/CD172a contributes to eosinophil homeostasis by regulating the degranulation in these cells, with substantial effects on their survival.

Materials and Methods

Mice

Female 6–12 wk-old BALB/c and C57BL/6 mice (SLC, Hamamatsu, Japan) were used. A C57BL/6 mouse strain expressing a mutant SIRPα/CD172a lacking most of its cytoplasmic domain (25) was backcrossed onto the BALB/c background for >10 generations (hereafter referred to as SIRPα Cyto$^{-/-}$). The CD47$^{-/-}$ mice on the C57BL/6 background were kindly provided by Dr. Per-Arne Oldenborg (Umea University, Umea, Sweden). All animal experiments were performed under an experimental protocol approved by the Ethics Review Committee for Animal Experimentation of Osaka University Graduate School of Medicine.

Reagents

O-phenylenediamine, cetyltrimethylammonium bromide, and calcium ionophore A23187 were purchased from Sigma-Aldrich (St. Louis, MO). The stock solution of A23187 (10 mM) was prepared in DMSO, and subsequent dilutions were prepared in RPMI 1640 without phenol red (Invitrogen Life Technologies, Carlsbad, CA). Recombinant murine stem cell factor, recombinant murine Flt3 ligand, and recombinant murine IL-5 were all purchased from PeproTech (Rocky Hill, NJ) and used at the concentrations described previously (26). Recombinant murine IL-25 was from R&D Systems.

Cell isolation

The small intestine was isolated, and after removal of the fat tissue and Peyer's patches, the intestine was opened longitudinally, rinsed in cold 5 mM EDTA in PBS, and cut into 1–2-cm lengths. The epithelial cell layer was removed by vigorous stirring in FACS buffer (PBS containing 10% FCS, 20 mM HEPES, 100 U/ml penicillin, 100 μg/ml streptomycin, 1 mM sodium pyruvate, and 10 mM EDTA) for 20 min at 37°C. After shaking in PBS, the intestinal fragments were incubated in complete RPMI 1640 medium for 10 min at room temperature (RT), minced, and digested in 400 U/ml collagenase D and 10 μg/ml DNase I (Roche, Mannheim, Germany) at 37°C for 45 min with continuous stirring. The cell suspension was filtered through a 40-μm cell strainer and subjected to 40%/75% Percoll (Amersham Biosciences) density-gradient centrifugation. Cells at the interface (hereafter referred to as "light-density cells") were collected, washed, and used for phenotypic analysis, immunoprecipitation, eosinophil degranulation assay, or culture. BM cells were collected by flushing the femurs and tibiae with complete RPMI 1640 medium. The red cells in the BM and blood were lysed with ACK lysis buffer (0.15 M NH_4Cl, 10 mM $KHCO_3$, 0.1 mM Na_2EDTA [pH 7.3]), and the remaining leukocytes were subjected to enzymatic digestion, as described above for the lamina propria leukocytes, or used directly for phenotypic analysis. BM-derived eosinophils were obtained by culturing BM cells in the presence of the stem cell factor, Flt3 ligand, and IL-5, following a previously described method (26).

Generation of MY-1 and NVG-2 mAbs

Sprague-Dawley rats were immunized with an eosinophil-enriched cell fraction, obtained by sorting granulocytes (FSC^{high} and SSC^{high}) from the mouse small intestinal lamina propria by FACS. Two weeks after the last booster immunization, the popliteal lymph nodes were used to generate hybridomas, following standard methods. Hybridomas were grown in hypoxanthine–aminopterin–thymidine medium supplemented with IL-6, and the culture supernatants were screened for Abs reactive with small intestinal lamina propria eosinophils by flow cytometry. The MY-1 and NVG-2 mAbs were produced in ascitic fluid from ICR nu/nu mice. They were both determined to be of the IgG2a subclass and purified using protein G-affinity chromatography.

Cell lines

CHO cells stably expressing an active form of H-Ras (CHO-Ras cells) and those stably expressing mouse SIRPα/CD172a (CHO-Ras-SIRPα-ICR) were cultured in α-MEM medium (Sigma-Aldrich) supplemented with 10% FCS, 2 mM L-glutamine, 10 mM HEPES, 500 μg/ml Geneticin, and 500 μg/ml Zeocin, as previously described (27). COS-7 cells were maintained in DMEM supplemented with 10% heat-inactivated FCS, L-glutamine, and 0.1 mM nonessential amino acids at 37°C with 5% CO_2 and transfected with a pCMV-SPORT6 expression vector encoding mouse CD63 Ag (Invitrogen Life Technologies) to generate a stable cell line expressing CD63 on the cell surface.

Abs and flow cytometry

Unlabeled mAbs used in EPO-release experiments were anti-mouse sialic acid-binding Ig-like lectin F (Siglec F; 238047), anti-mouse PIR-B (326414) from R&D Systems, rat IgG2a isotype control (eBioscience), and MY-1. Abs used in flow cytometry were Alexa Fluor 647- or FITC-conjugated MY-1, Alexa Fluor 647- or FITC-conjugated NVG-2, anti-CD63 (MBL, Woburn, MA), and FITC-conjugated anti–CCR-3 (83101) from R&D Systems. PE-conjugated anti-Siglec F (E50-2440), PE-conjugated anti-CD125 (T21), allophycocyanin- or PE-conjugated anti-CD11c (HL3), and FITC-conjugated Annexin V were from BD Pharmingen. Allophycocyanin- or PE-conjugated anti-CD11b (M1/70) and FITC-conjugated rat IgG2a isotype control were from eBioscience. PE- or Alexa Fluor 647-conjugated rat IgG2a κ (RTK2758) isotype control Abs were from BioLegend. Biotin-conjugated P84 mAb was produced from hybridoma cells kindly provided by Dr. C.F. Lagenaur (University of Pittsburgh, Pittsburgh, PA). FcR blocking was performed using anti-CD16/32 (2.4G2) or mouse γ-globulins when necessary. After addition of a nucleic acid dye 7-aminoactinomycin D (7AAD), flow cytometric analysis was performed on a FACSCanto II (BD Biosciences) or Gallios (Beckman Coulter), and the data were processed with FlowJo (Tree Star) or Kaluza (Beckman Coulter) software. The geometric mean fluorescence intensity values of isotype control Abs were subtracted from those of specific Abs.

Immunoprecipitation, Western blot, and liquid chromatography mass spectrometry analysis

The MY-1 and NVG-2 mAbs were covalently linked to Sepharose beads (GE Healthcare) and used to immunoprecipitate Ags from lysates of lamina propria light-density cells. The immunoprecipitated Ag was washed in PBS containing 0.1% Triton X-100 and 500 mM NaCl, eluted with glycine-HCl (pH 2.5), neutralized immediately with 3 μl Tris-HCl (pH 9.0), and concentrated 10 times using a CC-105 centrifugal concentrator (Tomy Tech). Cell lysates and the immunoprecipitated materials were resuspended in 2× SDS PAGE sample buffer and separated on a 5–20% SDS-PAGE gel under reducing or nonreducing conditions. After blotting, the filters were incubated with the MY-1 or NVG-2 mAbs, followed by HRP-conjugated goat anti-rat IgG, and detected with ECL Western blotting detection reagents (GE Healthcare). An additional gel was stained with the Sypro Ruby protein gel stain (Invitrogen Life Technologies), and the protein band was isolated and digested with trypsin. The eluted peptides were analyzed by liquid chromatography mass spectrometry (LC/MS). The mass spectrometry data were compared with primary sequence databases using the Mascot search (http://www.matrixscience.com).

Eosinophil-degranulation assay

Small intestinal lamina propria light-density cells (5×10^5 cells/well, 30 ± 5% eosinophils) and in vitro-differentiated BM-derived eosinophils (2.5×10^5 cells/well, >90% eosinophils) were assayed for EPO release following a previously described method that measured extracellular EPO (28). The cells were resuspended in RPMI 1640 medium without phenol red and

incubated with 50 μg/ml mouse γ-globulins for 15 min at RT. The cells were then incubated with 2.5 μg/ml MY-1, anti–Siglec-F, anti–PIR-B, rat IgG2a isotype control, or the indicated Ab combination for 10 min at RT. After washing with RPMI 1640 medium without phenol red, the cells were incubated with 2.5 μg/ml goat anti-rat IgG for 10 min at RT. After the removal of unbound Abs, the cells were stimulated with 10 μM A23187 (29) for 30 min at 37°C in a 5% CO_2 incubator. Subsequently, a substrate solution (0.4 M Tris-HCl, 0.2 mM *o*-phenylenediamine, 0.005% H_2O_2) was added, and the mixture was left for 15 min at RT before stopping the enzymatic reaction with cold 4 M H_2SO_4. The total EPO activity was determined from cells lysed in 0.3 M sucrose containing 0.22% cetyltrimethylammonium bromide and 0.2% Triton X-100. The absorbance was determined at 492 nm in a microplate reader, and the data are presented as the percentage of total EPO activity in lysed cells.

Immunofluorescence staining

Cryosections of the small intestine and spleen were blocked with 10% FCS in PBS containing 20 μg/ml mouse γ-globulins for 12 h at 4°C. The sections were stained with 2 μg/ml rat anti-mouse MBP mAb (kindly provided by D.J. Lee, Mayo Clinic, Scottsdale, AZ) for 1 h at RT, followed by Alexa Fluor 594-conjugated goat anti-rat IgG. After a second blocking with 10 μg/ml rat IgG, the sections were stained with FITC-labeled anti-CD63 (NVG-2 mAb) or Alexa Fluor 647-conjugated MY-1, followed by the nucleic acid dye Hoechst 33342. Apoptotic eosinophils were detected by TUNEL, using the In Situ Cell Death Detection Kit (Roche). Pictures were acquired by an Olympus FV-1000 confocal laser-scanning microscope.

Induction of Th2-type inflammation

IL-25 was administered i.p. (400 ng/mouse) daily for 3 d (30), and the peritoneal cells and tissues were collected 24 h after each treatment.

Statistical analysis

Flow cytometry data were collected from individual mice or from pooled samples from three to five mice. In the EPO-release experiments, the mean ± SD was calculated from the data collected from six to eight wells per treatment, and the experiment was repeated at least three times. Significant differences were determined using the Student *t* test. Statistical analysis was performed with GraphPad Prism 5 software (GraphPad).

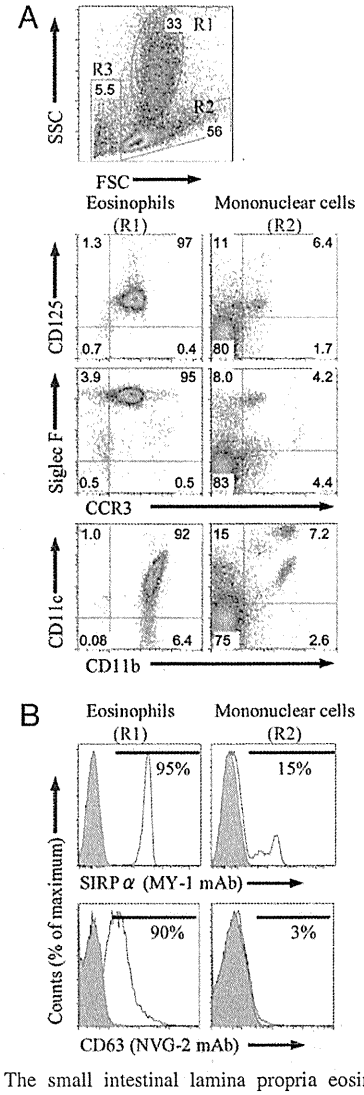

FIGURE 1. The small intestinal lamina propria eosinophils express SIRPα/CD172a and CD63. *A*, The small intestinal lamina propria light-density cells of naive BALB/c mice were stained with FITC-conjugated anti–CCR-3 and anti-CD11b, PE-conjugated anti-CD125 (IL-5Rα), anti-Siglec F, or anti-CD11c and analyzed by flow cytometry. *B*, The expression levels of SIRPα/CD172a and CD63 in the small intestinal lamina propria eosinophils were determined using Alexa Fluor 647-conjugated MY-1 or NVG-2 mAbs, respectively. Numbers inside the outlined areas or within each quadrant indicate the percentage of gated cells. Data are from one experiment representative of more than three with three mice each.

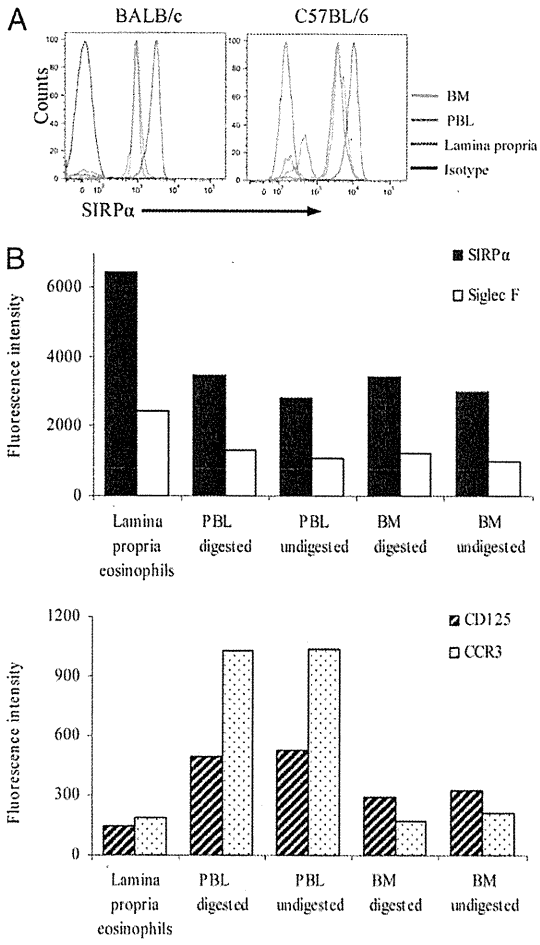

FIGURE 2. SIRPα/CD172a is more abundantly expressed in intestinal eosinophils than in BM or PBL eosinophils. *A*, Flow cytometry of the BM, PBL, and small intestinal lamina propria eosinophils from BALB/c and C57BL/6 mice, stained with Alexa Fluor 647-conjugated MY-1 (anti-SIRPα/CD172a). *B*, Geometric mean fluorescence intensity values of SIRPα/CD172a, Siglec F, CD125, and CCR-3 in BM and PBL eosinophils that had been subjected to treatment with collagenase D and DNase I, similar to that used for the lamina propria eosinophils. Data are from one experiment representative of three with three mice each.

Results

Eosinophils express SIRPα/CD172a and CD63 in the small intestinal lamina propria

Analysis of the small intestinal lamina propria light-density cells by flow cytometry indicated the presence of at least three main cell populations based on the forward light scatter (FSC)/side scatter (SSC) pattern of live cells: a granulocyte population with medium to high SSC (R1; 33 ± 5%), a mononuclear cell population with low SSC (R2; 56 ± 4%), and a minor cell population with low FSC/SSC (R3; 5.5 ± 7%) (Fig. 1*A*). Staining with mAbs against CCR3, IL-5Rα, and Siglec F verified that >90% of the granulocytes in the R1 fraction were eosinophils expressing all three of these markers. The majority of the R2 cells (>80%) were negative for CCR3, IL-5Rα, and Siglec F, although there were minor cell populations with the phenotype of $CCR3^-$ IL-$5R\alpha^+$ (11%), $CCR3^+$ IL-$5R\alpha^+$ (6.4%), $CCR3^+$ Siglec F^- (4.3%), $CCR3^-$ Siglec F^+ (8%), and $CCR3^+$ Siglec F^+ (4%), some of which might represent immature-type eosinophils. Additional staining indicated that almost all of the cells in the R1 gate (eosinophil-dominant subpopulation) expressed the integrin CD11c and reacted with two novel mAbs, MY-1 and NVG-2, which were generated against mouse eosinophils from the small intestinal lamina propria (see *Materials and Methods*). The lamina propria eosinophils had a high reactivity with MY-1 (95%) and a low, but significant, reactivity with NVG-2 (90%) (Fig. 1*B*), whereas the mononuclear cells in the R2 gate showed only minor or no reactivity with these mAbs.

When the Ags recognized by the mAbs MY-1 and NVG-2 were analyzed by Western blotting, MY-1 was found to recognize a major band with a molecular mass of ~100–120 kDa and a minor band of ~40 kDa, whereas NVG-2 reacted with a band of ~60–65 kDa in lamina propria cell lysates (Supplemental Fig. 1*A*). LC/MS analysis indicated that the major band recognized by MY-1 was an immune-inhibitory protein, SIRPα/CD172a (score 96.29, p = 5.00E−15), whereas NVG-2 reacted with tetraspanin CD63 (score 33, p = 4.19E−05), which appears on degranulating leukocytes. Confirming these data, the MY-1 mAb also reacted with CHO-Ras cells stably expressing mouse SIRPα/CD172a, as did a commercially available anti-SIRPα/CD172a mAb P84, in immunofluorescence and flow cytometric analyses (Supplemental Fig. 1*B*, 1*C*). The NVG-2 mAb reacted with COS-7 cells expressing the mouse CD63 Ag, as did a commercially available anti-CD63 (MBL) Ab (Supplemental Fig. 1*D*). Collectively, these results

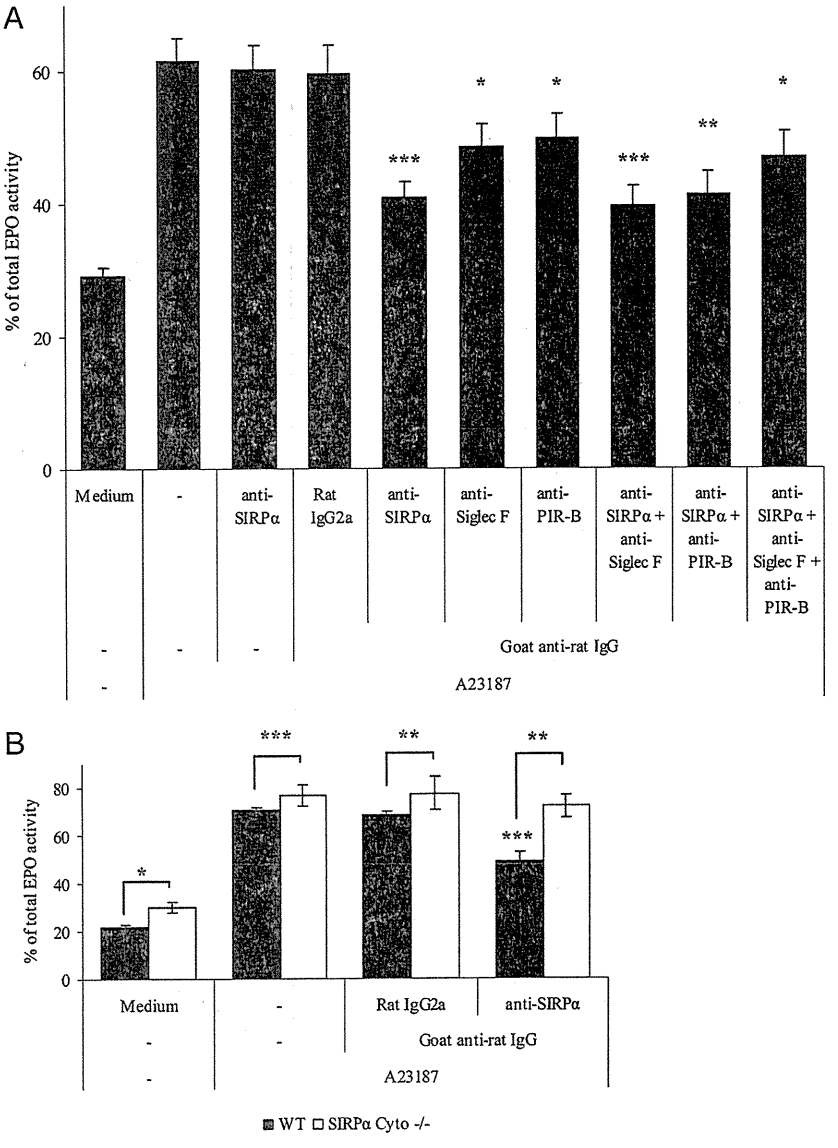

FIGURE 3. Cross-linking of SIRPα/CD172a on eosinophils leads to an inhibition of peroxidase release. *A*, A23187 (10 μM)-induced EPO release from lamina propria eosinophils that had been pretreated with 2.5 μg/ml MY-1, anti-Siglec F, anti–PIR-B, rat IgG2a isotype control, or the indicated Ab combinations, with or without subsequent cross-linking with 2.5 μg/ml goat anti-rat IgG. Data are presented as the percentage of total EPO activity from lysed cells. *B*, EPO release from the lamina propria eosinophils of WT and SIRPα $Cyto^{-/-}$ mice treated as in *A* and stimulated with 10 μM A23187. Data are the mean values ± SD of six to eight wells from one experiment representative of three. Statistical significance of the differences was determined using the Student unpaired t test. $*p < 0.05$, $**p < 0.001$, $*** p < 0.0001$, compared with rat IgG2a isotype control Ab or between the indicated groups.

indicated that eosinophils in the lamina propria of the small intestine express SIRPα/CD172a at a high level and CD63 at a low, but significant, level.

SIRPα/CD172a is more abundantly expressed in intestinal eosinophils than in BM or PBL eosinophils

We next asked whether SIRPα/CD172a is expressed in eosinophils in other tissues. As shown in Fig. 2*A*, SIRPα/CD172a expression was comparable between the BM and blood eosinophils, whereas its expression was substantially higher in the lamina propria eosinophils in BALB/c and C57BL/6 mice (Fig. 2*A*). To exclude the possibility that the higher levels of SIRPα/CD172a observed in lamina propria eosinophils were due to differences in the isolation method, we subjected PBL and BM leukocytes to an isolation method similar to that used for the lamina propria cells and analyzed the expression of SIRPα/CD172a comparatively with other markers. Subtracting the geometric mean fluorescence intensity values of isotype control Abs from the values of the specific Abs, we found that the collagenase treatment did not significantly alter the expression levels of SIRPα/CD172a, Siglec F, CD125 (IL-5Rα), or CCR3 in the PBL or BM eosinophils. Furthermore, the intestinal eosinophils expressed both SIRPα/CD172a and Siglec F at higher levels and CD125 and CCR3 at lower levels than did those obtained from the PBL and BM (Fig. 2*B*).

Cross-linking of SIRPα/CD172a leads to the inhibition of EPO release

To understand the role of SIRPα/CD172a in intestinal eosinophils, we asked whether cross-linking SIRPα/CD172 on the cell surface has any effect on the A23187-induced release of EPO (28). As

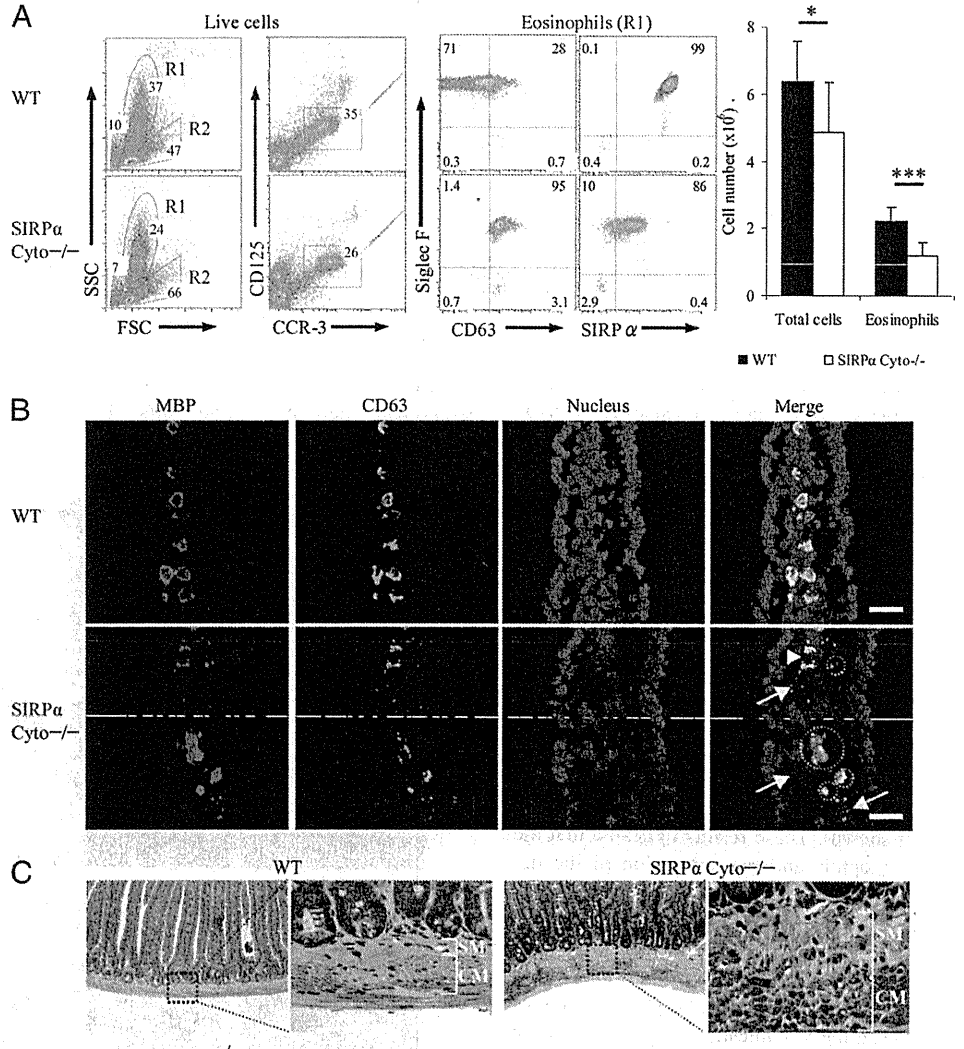

FIGURE 4. Mice expressing SIRPα Cyto$^{-/-}$ show increased eosinophil degranulation and lamina propria remodeling. *A*, Flow cytometry of lamina propria leukocytes from WT and SIRPα Cyto$^{-/-}$ mice stained with anti–CCR-3, anti-CD125, anti-Siglec F, anti-SIRPα/CD172a (MY-1), and anti-CD63 (NVG-2) mAbs or rat IgG isotype control Abs. Numbers inside the outlined areas or within each quadrant indicate the percentage of gated cells. The total number of lamina propria light-density cells and of eosinophils in WT and SIRPα Cyto$^{-/-}$ mice is shown in the *far right panel*. Statistical significance of the differences was determined using the Student unpaired *t* test. $*p < 0.05$, $***p < 0.0001$. Data are from one experiment representative of more than three with three mice per group. *B*, Confocal laser-scanning microscopy images of frozen sections from the small intestine of WT and SIRPα Cyto$^{-/-}$ mice immunostained for MBP (red), CD63 (green), and nuclei (Hoechst 33342, blue). Dotted circles demarcate MBP$^+$CD63$^+$ amorphous structures compatible with clusters of free extracellular granules. Arrows indicate free MBP$^+$CD63$^+$ granules, and white arrowhead indicates MBP$^+$CD63$^+$ granules apparently in the cytoplasm of mononuclear leukocytes. Scale bars, 20 μm. Data are from one experiment representative of more than three. *C*, Paraffin wax-embedded sections of the small intestine of WT and SIRPα Cyto$^{-/-}$ mice stained with Masson's trichrome. Collagen is stained blue, and white brackets indicate the submucosa (SM) and circular muscle layer (CM). Original magnification ×200 (*first* and *third panels*) and ×1000 (*second* and *fourth panels*). Data are from one experiment representative of two.

shown in Fig. 3*A*, intestinal eosinophils obtained from unperturbed wild-type (WT) mice showed a modest, but significant, reduction in EPO release upon the cross-linking of SIRPα/CD172a. In contrast, intestinal eosinophils from mice expressing SIRPα Cyto$^{-/-}$, which is a mutated SIRPα/CD172a that lacks most of its cytoplasmic domain and, hence, has no signal-transducing ability, did not show a significant reduction in EPO release after SIRPα/CD172a cross-linking (Fig. 3*B*); instead, the mutant cells showed a tendency to release more EPO with or without stimulation. This inhibitory effect on EPO release in WT eosinophils was found only when the cells were treated with anti-SIRPα/CD172a mAb, followed by a secondary Ab, but not with anti-SIRPα/CD172a mAb alone (Fig. 3*A*). A comparable inhibition of EPO release was observed by SIRPα/CD172a cross-linking in WT BM-derived eosinophils (data not shown). These findings are consistent with the hypothesis that SIRPα/CD172a negatively regulates eosinophil degranulation via its cytoplasmic domain.

The cross-linking of other inhibitory receptors, Siglec F and PIR-B, also inhibited eosinophil degranulation at low levels, and the simultaneous cross-linking of SIRPα/CD172a enhanced the inhibition by either of these receptors slightly; cross-linking all three receptors did not enhance the inhibition further (Fig. 3*A*). These results suggested that there are multiple arms of regulation in eosinophil degranulation in the intestine, and these inhibitory receptors may act independently.

Mice expressing SIRPα Cyto$^{-/-}$ show increased eosinophil degranulation and lamina propria remodeling

We next asked whether the absence of SIRPα/CD172a-mediated inhibitory signals compromises eosinophil homeostasis in vivo. As shown in Fig. 4*A*, we found a decrease in SSC^{high} light-density cells in the lamina propria of SIRPα Cyto$^{-/-}$ mice compared with WT mice (24% versus 37%), which mainly reflected a decrease in eosinophils, as revealed by staining with anti-CCR3 and anti-CD125 mAbs. Manual counting of live cells obtained from the small intestinal lamina propria confirmed that there was a lower recovery of total cells and eosinophils from the SIRPα Cyto$^{-/-}$ mice. Eosinophils from the small intestine of the SIRPα Cyto$^{-/-}$ mice showed increased expression of the tetraspanin CD63 and reduced levels of the mutated SIRPα/CD172a. The cells in the R2 fraction, which were mainly macrophages and dendritic cells expressing SIRPα/CD172a, did not show obvious changes in cell number, but they showed reduced expressions of MHC class II and F4/80 in SIRPα Cyto$^{-/-}$ mice compared with WT mice (data not shown). These results indicated that the number of intestinal eosinophils and the expression of the degranulation marker CD63 were altered in mice expressing a mutant SIRPα/CD172a protein.

A close examination of the small intestine of the SIRPα Cyto$^{-/-}$ mice confirmed the increased eosinophil degranulation, with markedly more MBP^{+} CD63^{+} granules and amorphous structures in the lamina propria than in the WT intestine (Fig. 4*B*). Some of the MBP^{+} CD63^{+} granules in the SIRPα Cyto$^{-/-}$ lamina propria were found within the cytoplasm of other leukocytes, indicating that the eosinophils' granular contents were released extracellularly and phagocytosed by other cells. Masson's trichrome staining showed increased collagen deposition in the submucosa and smooth muscle hypertrophy (Fig. 4*C*). Taken together, these data indicated that, in the absence of SIRPα/CD172a signaling, intestinal eosinophils had an increased tendency to degranulate, leading to reduced eosinophil viability and increased expression of the degranulation marker CD63. The lamina propria showed increased tissue remodeling under steady-state conditions.

CD47$^{-/-}$ mice show increased eosinophil degranulation and reduced numbers of lamina propria eosinophils

Given that SIRPα/CD172a transmits negative signals upon ligation by the transmembrane glycoprotein CD47 (31), which is expressed in a number of cell types (32), including intestinal epithelial cells (33), we examined whether CD47$^{-/-}$ mice recapitulate the changes observed in the SIRPα Cyto$^{-/-}$ mice. In this experiment, because the only CD47$^{-/-}$ mice available were on the C57BL/6 background, we made the comparisons using SIRPα Cyto$^{-/-}$ mice on the C57BL/6 background, instead of the BALB/c background. As shown in Fig. 5*A*, both CD47$^{-/-}$ and SIRPα Cyto$^{-/-}$ mice showed a substantial reduction in the number of eosinophils and increased degranulation in the lamina propria compared with age- and sex-matched WT mice. In the spleen, the number of degranulating eosinophils was also increased in both the SIRPα Cyto$^{-/-}$ and CD47$^{-/-}$ mice (Fig. 5*B*). These results are consistent with the hypothesis that a lack of signals provided by the SIRPα/CD172a–CD47 interaction leads to increased eosinophil degranulation and reduced eosinophil numbers in the intestine.

SIRPα/CD172a mutation negatively affects eosinophil survival

We next asked whether eosinophils show decreased survival in the absence of SIRPα/CD172a signaling. The small intestinal lamina propria light-density cells from SIRPα Cyto$^{-/-}$ mice showed a higher incidence of cell death, irrespective of the presence of IL-5, after 24 h of culture (Fig. 6*A*). In the absence of IL-5, SIRPα Cyto$^{-/-}$ lamina propria eosinophils showed increased early (7AAD^{-} Annexin V^{+} cells; 13% versus 9.8%) and late (7AAD^{+} Annexin V^{+} cells; 50% versus 34%) apoptotic cell death compared with their WT counterparts. IL-5 showed little survival

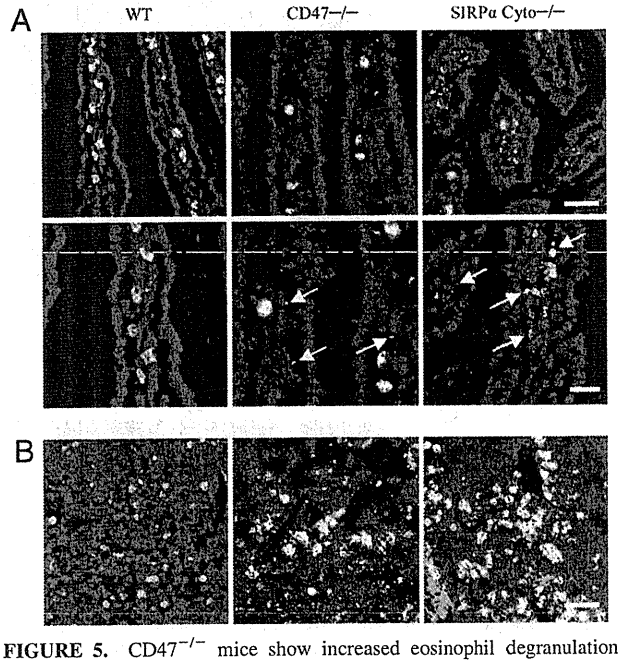

FIGURE 5. CD47$^{-/-}$ mice show increased eosinophil degranulation and reduced numbers of lamina propria eosinophils. *A*, Merged images of frozen sections from the small intestine of CD47$^{-/-}$ and SIRPα Cyto$^{-/-}$ mice on the C57BL/6 background, immunostained for MBP (red), CD63 (green), and nuclei (Hoechst 33342, blue), acquired by a confocal laser-scanning microscope. Arrows indicate MBP^{+}CD63^{+} extracellular granules. Scale bars, 40 μm (*upper panels*) and 20 μm (*lower panels*). *B*, Merged images of frozen sections from the spleen of CD47$^{-/-}$ and SIRPα Cyto$^{-/-}$ mice on the C57BL/6 background, immunostained as in *A*. Scale bar, 40 μm. Data are from one experiment representative of three.

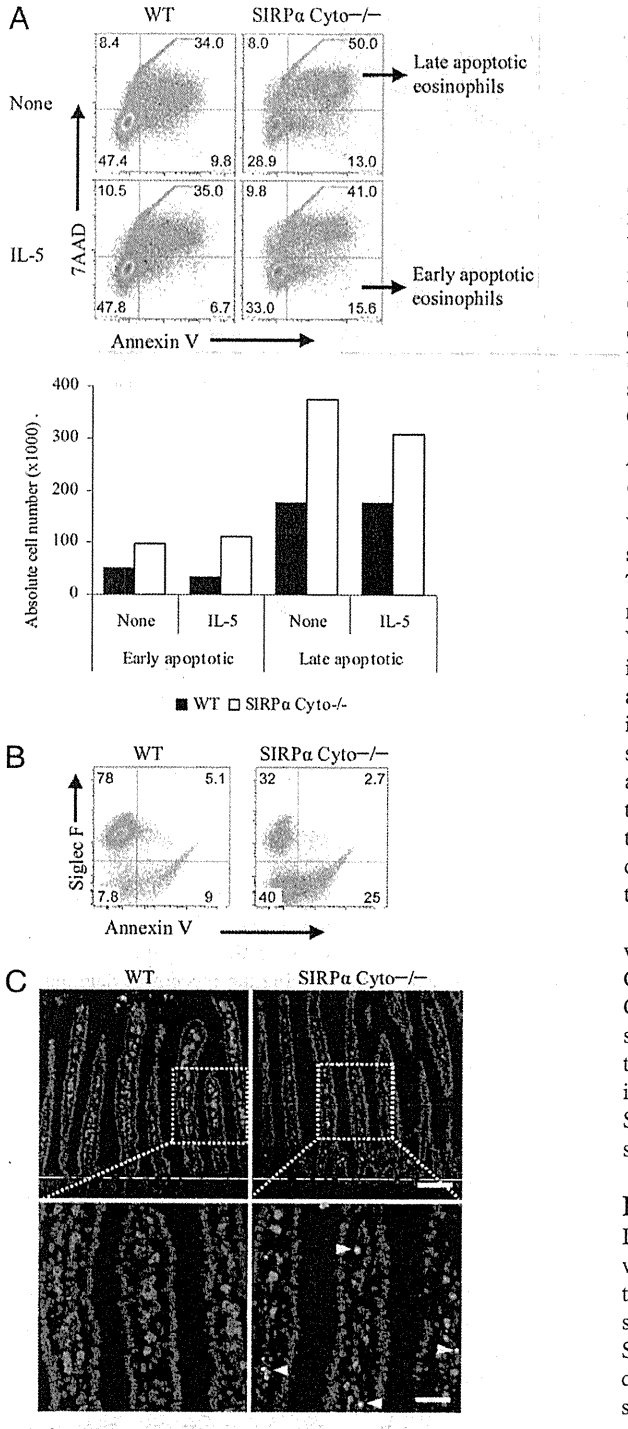

FIGURE 6. SIRPα/CD172a mutation negatively affects eosinophil survival. *A*, The survival of small intestinal lamina propria leukocytes was analyzed 24 h after culture in complete RPMI 1640 medium in the presence or absence of 10 ng/ml IL-5. The cells were stained with FITC-conjugated Annexin V and the nucleic acid dye 7AAD and analyzed by FACS. *Lower panel*, The absolute number of early and late apoptotic eosinophils. Data are from one experiment representative of three. *B*, Flow cytometry of small intestinal lamina propria eosinophils stained with a PE-conjugated anti-Siglec F mAb and FITC-conjugated Annexin V. Numbers within each quadrant indicate the percentage of gated cells. Data are from one experiment representative of more than three. *C*, Merged images of frozen sections from the small intestine of WT and SIRPα Cyto$^{-/-}$ mice stained with TUNEL (green) and anti-MBP (red) and acquired by a confocal laser-scanning microscope. Arrowheads indicate TUNEL^{+} eosinophils, which appeared smaller than WT eosinophils. The extracellular granules and amorphous structures shown in Figs. 4 and 5 were present but not readily visible without CD63 staining. Scale bars, 100 μm (*upper panels*) and 40 μm (*lower panels*). Data are from one experiment representative of two.

effect on cultured lamina propria eosinophils and yielded only a small reduction in early (9.8% versus 6.7%) and late (50% versus 41%) apoptosis in WT and SIRPα Cyto$^{-/-}$ eosinophils, respectively (Fig. 6*A*, *upper panels*). These observations were also apparent when the absolute cell numbers were compared (Fig. 6*A*, *lower panels*). A similar tendency was observed after 48 h of culture (data not shown). Furthermore, the small intestinal eosinophils from SIRPα Cyto$^{-/-}$ mice showed increased Annexin V binding at the time of cell harvest compared with those from WT mice (total Annexin V^{+} eosinophils: 27.7% versus 13.1%) (Fig. 6*B*). Finally, MBP^{+} TUNEL^{+} apoptotic eosinophils were frequently observed in the small intestine of SIRPα Cyto$^{-/-}$ mice but not WT mice (Fig. 6*C*). These results demonstrated that eosinophil survival was compromised in the absence of SIRPα/CD172a signaling, both in vitro and in vivo.

Reduced survival of eosinophils in the absence of SIRPα/CD172a signaling in inflammation

We next asked whether the absence of appropriate SIRPα/CD172a signaling would affect eosinophil homeostasis in inflammation. To this end, we injected IL-25 i.p. into WT and SIRPα Cyto$^{-/-}$ mice to induce a Th2-type inflammatory response (30, 34). The WT mice showed a significant increase in eosinophils in the small intestinal lamina propria after 3 d of daily IL-25 administration, and a substantial proportion of the eosinophils was degranulating in the villus (Fig. 7*A*). In contrast, the SIRPα Cyto$^{-/-}$ mice showed a much lower frequency of lamina propria eosinophils but a marked increase in MBP^{+} CD63^{+} amorphous material outside the intestinal villi (Fig. 7*A*). These observations indicated that, in the absence of SIRPα/CD172a signaling, the eosinophils rapidly degranulated, and their cytoplasmic contents were released into the lumen in the inflamed intestine.

Corroborating these observations, marked eosinophil infiltration was seen in the peritoneal cavity in both the WT and SIRPα Cyto$^{-/-}$ mice upon IL-25 administration (Fig. 7*B*). The SIRPα Cyto$^{-/-}$ mice showed a prominent reduction in Siglec F expression and a concomitant increase in Annexin V-binding cells in the R1, but not the R2, fraction (Fig. 7*B*), indicating an increase in dying eosinophils. Collectively, these results indicated that SIRPα/CD172a signaling significantly contributes to eosinophil survival in inflammation.

Discussion

In this study, through the generation and use of two novel mAbs, we identified an inhibitory receptor, SIRPα/CD172a (35), and the tetraspanin CD63 (36) as proteins expressed on the surface of small intestinal lamina propria eosinophils. We also showed that SIRPα/CD172a regulates eosinophil homeostasis by inhibiting degranulation, a mechanism that seems to increase eosinophil survival under both physiological and inflammatory conditions.

SIRPα/CD172a (also known as SHPS-1, P84, or BIT), possesses two ITIM motifs in its cytoplasmic domain that can transmit negative signals in various cellular events, including proliferation (35, 37), cytoskeletal reorganization and cell motility (38), and phagocytosis and oxidative burst (25, 39, 40). In the current study, we found that cross-linking SIRPα/CD172a on lamina propria eosinophils significantly inhibited calcium

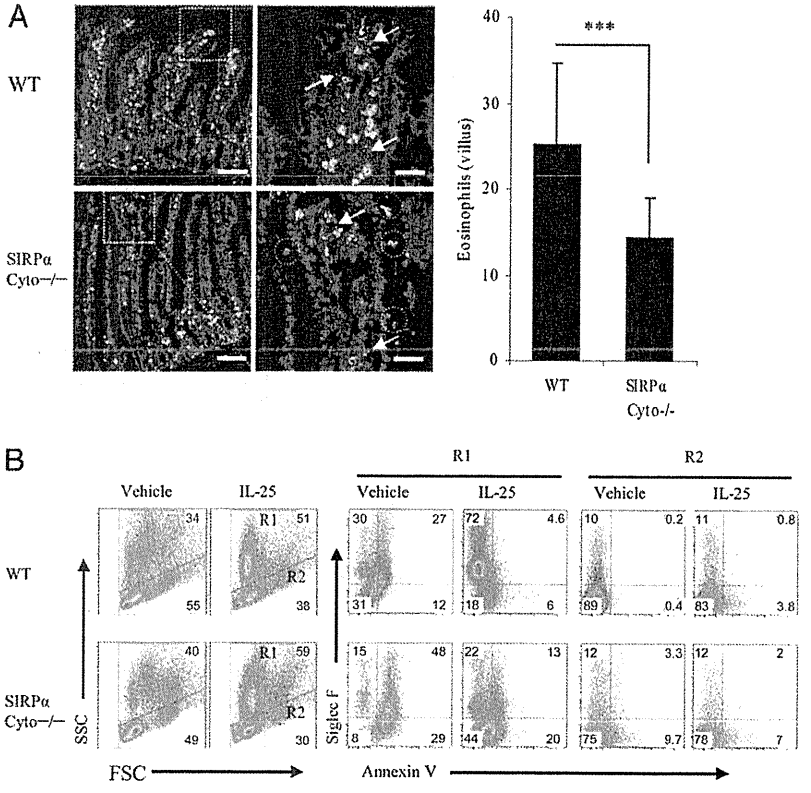

FIGURE 7. Reduced survival of eosinophils in the absence of SIRPα/CD172a signaling in inflammation. *A*, Merged images of frozen sections from the small intestine of WT and SIRPα Cyto$^{-/-}$ mice treated with IL-25 and stained with Abs to MBP (red), CD63 (green), and nuclei (Hoechst 33342, blue), acquired by a confocal laser-scanning microscope. Dotted circles indicate MBP$^+$CD63$^+$ amorphous structures shed from the lamina propria. Arrows indicate MBP$^+$CD63 extracellular granules. Scale bars, 100 μm (*left panels*) and 40 μm (*right panels*). *Right panel*, The number of eosinophils in 20 villus/crypt units was counted; data shown are eosinophils/villus (mean ± SD). ***$p < 0.0001$, Student unpaired *t* test. *B*, Flow cytometry of the total peritoneal cells from WT and SIRPα Cyto$^{-/-}$ mice collected 72 h after IL-25 or saline treatment and stained with PE-conjugated anti-Siglec F and FITC-conjugated Annexin V. Numbers inside the outlined areas or within each quadrant indicate the percentage of gated cells. Data are from one experiment representative of three.

ionophore-induced EPO release (Fig. 3). Although this inhibition was modest, it was consistently observed in both intestinal eosinophils and BM-derived eosinophils from normal mice but not in those from SIRPα Cyto$^{-/-}$ mice expressing a mutant SIRPα/CD172a that lacks most of its cytoplasmic domain, consistent with the notion that SIRPα/CD172a inhibits eosinophil degranulation via its cytoplasmic domain. The lower expression of the SIRPα/CD172a protein in SIRPα Cyto$^{-/-}$ eosinophils might have contributed to the lack of inhibition of EPO release upon cross-linking. However, the finding that SIRPα Cyto$^{-/-}$ eosinophils consistently showed a higher tendency to degranulate, even in the absence of cross-linking, argued against this possibility and instead indicated that they are more prone to degranulate than are their WT counterparts.

There are at least three possible explanations for the modest effect of the SIRPα/CD172a cross-linking. First, the SIRPα/CD172a-mediated degranulation inhibition seems to represent just one arm of multiple inhibitory pathways. As shown in Fig. 3*A*, the cross-linking of two other inhibitory receptors, Siglec F (41) and PIR-B, yielded a comparable or smaller degranulation inhibition, and the additional cross-linking of SIRPα/CD172a tended to increase the inhibition. Furthermore, other inhibitory receptors have been reported on the surface of eosinophils (42). Second, mouse eosinophils are much less susceptible to degranulation induction than are their human counterparts in vitro and in vivo (43). Third, eosinophils represented no more than one third of the light-density cell fraction used in this study, which might have decreased the sensitivity of the assay. Although the eosinophils could have been purified more by cell sorting, we deliberately used an eosinophil-enriched cell population without subjecting it to further purification, because the isolation method, per se, affected the degree of spontaneous eosinophil degranulation (Fig. 3).

The involvement of SIRPα/CD172a in regulating eosinophil degranulation was strongly supported by our in vivo study. Consistent with the hypothesis that the cytoplasmic domain of SIRPα/CD172a plays an inhibitory role in degranulation, the SIRPα Cyto$^{-/-}$ mice showed a reduced number of eosinophils in the small intestinal lamina propria and an increased surface expression of the degranulation marker CD63 (Fig. 4), which is normally present in the membrane of intracellular crystalloid granules and appears on the cell surface during the piecemeal degranulation of human eosinophils (17, 44). In addition, the SIRPα Cyto$^{-/-}$ mice showed an increased frequency of extracellular MBP$^+$CD63$^+$ granules and MBP$^+$CD63$^+$ amorphous materials in the lamina propria, increased collagen deposition in the submucosa, and smooth muscle hypertrophy in the jejunum, which are characteristic features of the increased tissue remodeling induced by eosinophil degranulation (45). Furthermore, the CD47$^{-/-}$ mice showed reduced numbers of lamina propria eosinophils and frequent MBP$^+$CD63$^+$ extracellular granules. Although MBP$^+$CD63$^+$ amorphous structures were not found in the lamina propria of the CD47$^{-/-}$ mice, they were observed in the spleen of these mice, where eosinophil degranulation was more prominent. These results provide strong support for the inhibitory role of SIRPα/CD172a in eosinophil degranulation.

Despite the increased eosinophil degranulation and tissue remodeling in the small intestine of the SIRPα Cyto$^{-/-}$ mice, we did not find significant inflammation or intestinal tissue damage resulting from the release of eosinophil granule proteins. This observation might be explained, in part, by a species difference, because mouse models of human asthma show only mild eosinophil degranulation (46). However, extensive eosinophil degranulation and pulmonary pathologies could be induced in double-transgenic mice expressing IL-5 and eotaxin-2 coordinately by mature T cells and lung epithelial cells, respectively (47), implying that in vivo eosinophil effector functions mediated by degranulation might involve multiple costimulatory receptor–ligand interactions. In addition, previous studies in man indicated that eosinophil granules are secreted extracellularly as intact membrane-bound structures and that external stimulation is required to elicit

secretion from the granules (14, 48). The small intestine may lack the endogenous activating signal necessary for the ejection of toxic granular contents from the released MBP^+CD63^+ granules, preventing any obvious tissue damage. In addition, given that some MBP^+CD63^+ granules were found within the cytoplasm of other types of cells, a substantial proportion of the released MBP^+ $CD63^+$ granules might have been rapidly taken up by phagocytes before they ejected toxic materials. Although it has been widely believed that eosinophil degranulation leads directly to tissue damage, these data collectively support the idea that, under certain conditions, eosinophil degranulation leads to tissue remodeling in the absence of noticeable inflammatory cell infiltration and the resulting tissue damage (43).

Eosinophils are terminally differentiated leukocytes that are believed to possess a limited ability to survive in tissues in the absence of survival-promoting cytokine signals (49), and cytokine signaling through the common γ-chain is reported to increase the survival of intestinal eosinophils (21). Although it is possible that inhibitory receptors inhibit these survival signals in eosinophils under certain situations (22), our results indicated that SIRPα/CD172a promotes eosinophil survival instead, because in vitro-cultured SIRPα $Cyto^{-/-}$ eosinophils showed reduced viability compared with WT eosinophils, and SIRPα $Cyto^{-/-}$ mice showed reduced intestinal eosinophils and eosinophils with increased Annexin V binding or $TUNEL^+$ staining (Fig. 6). Although IL-5 treatment seemed to have little effect on the survival of both WT and SIRPα $Cyto^{-/-}$ lamina propria eosinophils (Fig. 6*A*), this was probably due to the short time (24 h) of cell culture. Significant survival effects of IL-5 on WT lamina propria eosinophils were apparent when the cells were cultured for an extended period of time (48–72 h; data not shown). Although it remains to be analyzed whether SIRPα $Cyto^{-/-}$ lamina propria eosinophils respond favorably to the prosurvival signals of IL-5 in culture, technical difficulties with the isolation of sufficient numbers of viable SIRPα $Cyto^{-/-}$ eosinophils have impeded these experiments.

The reduced eosinophil survival was also obvious when inflammation was induced in SIRPα $Cyto^{-/-}$ mice by IL-25 administration. Taken together, these findings suggested that the absence of appropriate negative signaling via the cytoplasmic region of SIRPα/CD172a accelerated the rate of eosinophil cell death in vivo under steady-state or pathological conditions, probably because of their accelerated degranulation, and we excluded the possibility that this phenomenon was induced during the isolation process. Moreover, given that CD47, which binds SIRPα/CD172a to induce negative signals, is expressed in the basal aspect of intestinal epithelial cells, and that $CD47^{-/-}$ mice showed changes in the intestinal eosinophils that were very similar to those observed in the SIRPα $Cyto^{-/-}$ mice, the interaction of eosinophil SIRPα/CD172a and epithelial cell CD47 is likely to be involved in the regulation of eosinophil survival. A recent study indicated that both SIRPα/CD172a and CD47 are also important for dendritic cell homeostasis (50). In addition, not excluding the above-mentioned possibility, the absence of inhibitory signals provided by SIRPα/CD172a may also render eosinophils susceptible to death signals following the ligation of Fas (51) or of other receptors, such as Siglec F (52). The regulatory mechanism of eosinophil survival warrants further investigation.

A previous study indicated that human polymorphonuclear cell migration is regulated by CD47 through SIRPα/CD172a-dependent and -independent mechanisms (53). Abs against SIRPα/CD172a partially inhibited neutrophil migration across both human epithelial monolayers and collagen-coated filters, whereas Abs against CD47 inhibited neutrophil migration almost completely (53). In addition, mouse neutrophils deficient in CD47 showed reduced migration into the inflamed peritoneal cavity (40). However, in the current study, we found no evidence that SIRPα/CD172a regulates eosinophil migration. First, SIRPα $Cyto^{-/-}$ eosinophils efficiently migrated toward CCL24/eotaxin-2, as did WT eosinophils in vitro (data not shown). Second, although there was a slight delay in eosinophil recruitment into the peritoneal cavity in SIRPα $Cyto^{-/-}$ mice at 24 and 48 h after IL-25 injection, there was no such a delay at 72 h after inflammation induction. Instead, the only prominent finding at 72 h was the reduced viability of the infiltrated eosinophils (Fig. 7). Hence, our data do not support the role of SIRPα/CD172a in eosinophil migration regulation but rather support its role in eosinophil degranulation and cell survival.

In summary, we identified an inhibitory receptor, SIRPα/CD172a, and tetraspanin CD63 as proteins that are expressed by small intestinal lamina propria eosinophils. SIRPα/CD172a seems to play a role in inhibiting eosinophil degranulation, which leads to the prolongation of tissue-dwelling eosinophil survival. Given its prominent expression in human myeloid cells, including granulocytes (54), SIRPα/CD172a is also likely to be expressed in human eosinophils. If so, SIRPα/CD172a should be an interesting therapeutic target for eosinophil-associated diseases through the inhibition of eosinophil degranulation.

Acknowledgments

We thank Dr. Per-Arne Oldenborg for providing the $CD47^{-/-}$ mice and the members of Dr. Masaaki Murakami's laboratory for invaluable assistance with the LC/MS.

Disclosures

The authors have no financial conflicts of interest.

References

1. Rothenberg, M. E., and S. P. Hogan. 2006. The eosinophil. *Annu. Rev. Immunol.* 24: 147–174.
2. Matthews, A. N., D. S. Friend, N. Zimmermann, M. N. Sarafi, A. D. Luster, E. Pearlman, S. E. Wert, and M. E. Rothenberg. 1998. Eotaxin is required for the baseline level of tissue eosinophils. *Proc. Natl. Acad. Sci. USA* 95: 6273–6278.
3. Mishra, A., S. P. Hogan, J. J. Lee, P. S. Foster, and M. E. Rothenberg. 1999. Fundamental signals that regulate eosinophil homing to the gastrointestinal tract. *J. Clin. Invest.* 103: 1719–1727.
4. Ponath, P. D., S. Qin, T. W. Post, J. Wang, L. Wu, N. P. Gerard, W. Newman, C. Gerard, and C. R. Mackay. 1996. Molecular cloning and characterization of a human eotaxin receptor expressed selectively on eosinophils. *J. Exp. Med.* 183: 2437–2448.
5. Ponath, P. D., S. Qin, D. J. Ringler, I. Clark-Lewis, J. Wang, N. Kassam, H. Smith, X. Shi, J. A. Gonzalo, W. Newman, et al. 1996. Cloning of the human eosinophil chemoattractant, eotaxin. Expression, receptor binding, and functional properties suggest a mechanism for the selective recruitment of eosinophils. *J. Clin. Invest.* 97: 604–612.
6. Shin, E. H., Y. Osada, J. Y. Chai, N. Matsumoto, K. Takatsu, and S. Kojima. 1997. Protective roles of eosinophils in *Nippostrongylus brasiliensis* infection. *Int. Arch. Allergy Immunol.* 114(Suppl. 1): 45–50.
7. Voehringer, D., T. A. Reese, X. Huang, K. Shinkai, and R. M. Locksley. 2006. Type 2 immunity is controlled by IL-4/IL-13 expression in hematopoietic non-eosinophil cells of the innate immune system. *J. Exp. Med.* 203: 1435–1446.
8. Hogan, S. P., A. Mishra, E. B. Brandt, M. P. Royalty, S. M. Pope, N. Zimmermann, P. S. Foster, and M. E. Rothenberg. 2001. A pathological function for eotaxin and eosinophils in eosinophilic gastrointestinal inflammation. *Nat. Immunol.* 2: 353–360.
9. Forbes, E., T. Murase, M. Yang, K. I. Matthaei, J. J. Lee, N. A. Lee, P. S. Foster, and S. P. Hogan. 2004. Immunopathogenesis of experimental ulcerative colitis is mediated by eosinophil peroxidase. *J. Immunol.* 172: 5664–5675.
10. Filley, W. V., K. E. Holley, G. M. Kephart, and G. J. Gleich. 1982. Identification by immunofluorescence of eosinophil granule major basic protein in lung tissues of patients with bronchial asthma. *Lancet* 2: 11–16.
11. Malm-Erjefält, M., L. Greiff, J. Ankerst, M. Andersson, J. Wallengren, L. O. Cardell, S. Rak, C. G. Persson, and J. S. Erjefält. 2005. Circulating eosinophils in asthma, allergic rhinitis, and atopic dermatitis lack morphological signs of degranulation. *Clin. Exp. Allergy* 35: 1334–1340.
12. Carlson, M., Y. Raab, C. Peterson, R. Hällgren, and P. Venge. 1999. Increased intraluminal release of eosinophil granule proteins EPO, ECP, EPX, and cytokines in ulcerative colitis and proctitis in segmental perfusion. *Am. J. Gastroenterol.* 94: 1876–1883.

13. Saitoh, O., K. Kojima, K. Sugi, R. Matsuse, K. Uchida, K. Tabata, K. Nakagawa, M. Kayazawa, I. Hirata, and K. Katsu. 1999. Fecal eosinophil granule-derived proteins reflect disease activity in inflammatory bowel disease. *Am. J. Gastroenterol.* 94: 3513–3520.
14. Neves, J. S., and P. F. Weller. 2009. Functional extracellular eosinophil granules: novel implications in eosinophil immunobiology. *Curr. Opin. Immunol.* 21: 694–699.
15. Abu-Ghazaleh, R. I., T. Fujisawa, J. Mestecky, R. A. Kyle, and G. J. Gleich. 1989. IgA-induced eosinophil degranulation. *J. Immunol.* 142: 2393–2400.
16. Dubucquoi, S., P. Desreumaux, A. Janin, O. Klein, M. Goldman, J. Tavernier, A. Capron, and M. Capron. 1994. Interleukin 5 synthesis by eosinophils: association with granules and immunoglobulin-dependent secretion. *J. Exp. Med.* 179: 703–708.
17. Mahmudi-Azer, S., G. P. Downey, and R. Moqbel. 2002. Translocation of the tetraspanin CD63 in association with human eosinophil mediator release. *Blood* 99: 4039–4047.
18. Dyer, K. D., C. M. Percopo, Z. Xie, Z. Yang, J. D. Kim, F. Davoine, P. Lacy, K. M. Druey, R. Moqbel, and H. F. Rosenberg. 2010. Mouse and human eosinophils degranulate in response to platelet-activating factor (PAF) and lysoPAF via a PAF-receptor-independent mechanism: evidence for a novel receptor. *J. Immunol.* 184: 6327–6334.
19. Matsunaga, Y., H. Kido, K. Kawaji, K. Kamoshita, N. Katunuma, and T. Ogura. 1994. Inhibitors of chymotrypsin-like proteases inhibit eosinophil peroxidase release from activated human eosinophils. *Arch. Biochem. Biophys.* 312: 67–74.
20. Anwar, A. R., R. Moqbel, G. M. Walsh, A. B. Kay, and A. J. Wardlaw. 1993. Adhesion to fibronectin prolongs eosinophil survival. *J. Exp. Med.* 177: 839–843.
21. Carlens, J., B. Wahl, M. Ballmaier, S. Bulfone-Paus, R. Förster, and O. Pabst. 2009. Common gamma-chain-dependent signals confer selective survival of eosinophils in the murine small intestine. *J. Immunol.* 183: 5600–5607.
22. Munitz, A., I. Bachelet, R. Eliashar, A. Moretta, L. Moretta, and F. Levi-Schaffer. 2006. The inhibitory receptor IRp60 (CD300a) suppresses the effects of IL-5, GM-CSF, and eotaxin on human peripheral blood eosinophils. *Blood* 107: 1996–2003.
23. Munitz, A., M. L. McBride, J. S. Bernstein, and M. E. Rothenberg. 2008. A dual activation and inhibition role for the paired immunoglobulin-like receptor B in eosinophils. *Blood* 111: 5694–5703.
24. Ravetch, J. V., and L. L. Lanier. 2000. Immune inhibitory receptors. *Science* 290: 84–89.
25. Okazawa, H., S. Motegi, N. Ohyama, H. Ohnishi, T. Tomizawa, Y. Kaneko, P. A. Oldenborg, O. Ishikawa, and T. Matozaki. 2005. Negative regulation of phagocytosis in macrophages by the CD47-SHPS-1 system. *J. Immunol.* 174: 2004–2011.
26. Dyer, K. D., J. M. Moser, M. Czapiga, S. J. Siegel, C. M. Percopo, and H. F. Rosenberg. 2008. Functionally competent eosinophils differentiated ex vivo in high purity from normal mouse bone marrow. *J. Immunol.* 181: 4004–4009.
27. Motegi, S., H. Okazawa, Y. Murata, Y. Kanazawa, Y. Saito, H. Kobayashi, H. Ohnishi, P. A. Oldenborg, O. Ishikawa, and T. Matozaki. 2008. Essential roles of SHPS-1 in induction of contact hypersensitivity of skin. *Immunol. Lett.* 121: 52–60.
28. Adamko, D. J., Y. Wu, G. J. Gleich, P. Lacy, and R. Moqbel. 2004. The induction of eosinophil peroxidase release: improved methods of measurement and stimulation. *J. Immunol. Methods* 291: 101–108.
29. Kirino, Y., M. Mio, and C. Kamei. 2000. Regulatory mechanism of eosinophil peroxidase release from guinea pig eosinophils. *Jpn. J. Pharmacol.* 83: 293–299.
30. Neill, D. R., S. H. Wong, A. Bellosi, R. J. Flynn, M. Daly, T. K. Langford, C. Bucks, C. M. Kane, P. G. Fallon, R. Pannell, et al. 2010. Nuocytes represent a new innate effector leukocyte that mediates type-2 immunity. *Nature* 464: 1367–1370.
31. Jiang, P., C. F. Lagenaur, and V. Narayanan. 1999. Integrin-associated protein is a ligand for the P84 neural adhesion molecule. *J. Biol. Chem.* 274: 559–562.
32. Reinhold, M. I., F. P. Lindberg, D. Plas, S. Reynolds, M. G. Peters, and E. J. Brown. 1995. In vivo expression of alternatively spliced forms of integrin-associated protein (CD47). *J. Cell Sci.* 108: 3419–3425.
33. Mawby, W. J., C. H. Holmes, D. J. Anstee, F. A. Spring, and M. J. Tanner. 1994. Isolation and characterization of CD47 glycoprotein: a multispanning membrane protein which is the same as integrin-associated protein (IAP) and the ovarian tumour marker OA3. *Biochem. J.* 304: 525–530.
34. Fort, M. M., J. Cheung, D. Yen, J. Li, S. M. Zurawski, S. Lo, S. Menon, T. Clifford, B. Hunte, R. Lesley, et al. 2001. IL-25 induces IL-4, IL-5, and IL-13 and Th2-associated pathologies in vivo. *Immunity* 15: 985–995.
35. Fujioka, Y., T. Matozaki, T. Noguchi, A. Iwamatsu, T. Yamao, N. Takahashi, M. Tsuda, T. Takada, and M. Kasuga. 1996. A novel membrane glycoprotein, SHPS-1, that binds the SH2-domain-containing protein tyrosine phosphatase SHP-2 in response to mitogens and cell adhesion. *Mol. Cell. Biol.* 16: 6887–6899.
36. Metzelaar, M. J., P. L. Wijngaard, P. J. Peters, J. J. Sixma, H. K. Nieuwenhuis, and H. C. Clevers. 1991. CD63 antigen. A novel lysosomal membrane glycoprotein, cloned by a screening procedure for intracellular antigens in eukaryotic cells. *J. Biol. Chem.* 266: 3239–3245.
37. Kharitonenkov, A., Z. Chen, I. Sures, H. Wang, J. Schilling, and A. Ullrich. 1997. A family of proteins that inhibit signalling through tyrosine kinase receptors. *Nature* 386: 181–186.
38. Inagaki, K., T. Yamao, T. Noguchi, T. Matozaki, K. Fukunaga, T. Takada, T. Hosooka, S. Akira, and M. Kasuga. 2000. SHPS-1 regulates integrin-mediated cytoskeletal reorganization and cell motility. *EMBO J.* 19: 6721–6731.
39. Oldenborg, P. A., A. Zheleznyak, Y. F. Fang, C. F. Lagenaur, H. D. Gresham, and F. P. Lindberg. 2000. Role of CD47 as a marker of self on red blood cells. *Science* 288: 2051–2054.
40. Lindberg, F. P., D. C. Bullard, T. E. Caver, H. D. Gresham, A. L. Beaudet, and E. J. Brown. 1996. Decreased resistance to bacterial infection and granulocyte defects in IAP-deficient mice. *Science* 274: 795–798.
41. Zhang, J. Q., B. Biedermann, L. Nitschke, and P. R. Crocker. 2004. The murine inhibitory receptor mSiglec-E is expressed broadly on cells of the innate immune system whereas mSiglec-F is restricted to eosinophils. *Eur. J. Immunol.* 34: 1175–1184.
42. Munitz, A. 2010. Inhibitory receptors on myeloid cells: new targets for therapy? *Pharmacol. Ther.* 125: 128–137.
43. Lee, J. J., and N. A. Lee. 2005. Eosinophil degranulation: an evolutionary vestige or a universally destructive effector function? *Clin. Exp. Allergy* 35: 986–994.
44. Melo, R. C., S. A. Perez, L. A. Spencer, A. M. Dvorak, and P. F. Weller. 2005. Intragranular vesiculotubular compartments are involved in piecemeal degranulation by activated human eosinophils. *Traffic* 6: 866–879.
45. Humbles, A. A., C. M. Lloyd, S. J. McMillan, D. S. Friend, G. Xanthou, E. E. McKenna, S. Ghiran, N. P. Gerard, C. Yu, S. H. Orkin, and C. Gerard. 2004. A critical role for eosinophils in allergic airways remodeling. *Science* 305: 1776–1779.
46. Stelts, D., R. W. Egan, A. Falcone, C. G. Garlisi, G. J. Gleich, W. Kreutner, T. T. Kung, D. K. Nahrebne, R. W. Chapman, and M. Minnicozzi. 1998. Eosinophils retain their granule major basic protein in a murine model of allergic pulmonary inflammation. *Am. J. Respir. Cell Mol. Biol.* 18: 463–470.
47. Ochkur, S. I., E. A. Jacobsen, C. A. Protheroe, T. L. Biechele, R. S. Pero, M. P. McGarry, H. Wang, K. R. O'Neill, D. C. Colbert, T. V. Colby, et al. 2007. Coexpression of IL-5 and eotaxin-2 in mice creates an eosinophil-dependent model of respiratory inflammation with characteristics of severe asthma. *J. Immunol.* 178: 7879–7889.
48. Neves, J. S., S. A. Perez, L. A. Spencer, R. C. Melo, L. Reynolds, I. Ghiran, S. Mahmudi-Azer, S. O. Odemuyiwa, A. M. Dvorak, R. Moqbel, and P. F. Weller. 2008. Eosinophil granules function extracellularly as receptor-mediated secretory organelles. *Proc. Natl. Acad. Sci. USA* 105: 18478–18483.
49. Fulkerson, P. C., and M. E. Rothenberg. 2008. Origin, regulation and physiological function of intestinal oeosinophils. *Best Pract. Res. Clin. Gastroenterol.* 22: 411–423.
50. Saito, Y., H. Iwamura, T. Kaneko, H. Ohnishi, Y. Murata, H. Okazawa, Y. Kanazawa, M. Sato-Hashimoto, H. Kobayashi, P. A. Oldenborg, et al. 2010. Regulation by SIRPα of dendritic cell homeostasis in lymphoid tissues. *Blood* 116: 3517–3525.
51. Matsumoto, K., R. P. Schleimer, H. Saito, Y. Iikura, and B. S. Bochner. 1995. Induction of apoptosis in human eosinophils by anti-Fas antibody treatment in vitro. *Blood* 86: 1437–1443.
52. Zhang, M., T. Angata, J. Y. Cho, M. Miller, D. H. Broide, and A. Varki. 2007. Defining the in vivo function of Siglec-F, a CD33-related Siglec expressed on mouse eosinophils. *Blood* 109: 4280–4287.
53. Liu, Y., H. J. Bühring, K. Zen, S. L. Burst, F. J. Schnell, I. R. Williams, and C. A. Parkos. 2002. Signal regulatory protein (SIRPalpha), a cellular ligand for CD47, regulates neutrophil transmigration. *J. Biol. Chem.* 277: 10028–10036.
54. Seiffert, M., P. Brossart, C. Cant, M. Cella, M. Colonna, W. Brugger, L. Kanz, A. Ullrich, and H. J. Bühring. 2001. Signal-regulatory protein alpha (SIRPalpha) but not SIRPbeta is involved in T-cell activation, binds to CD47 with high affinity, and is expressed on immature CD34(+)CD38(−) hematopoietic cells. *Blood* 97: 2741–2749.

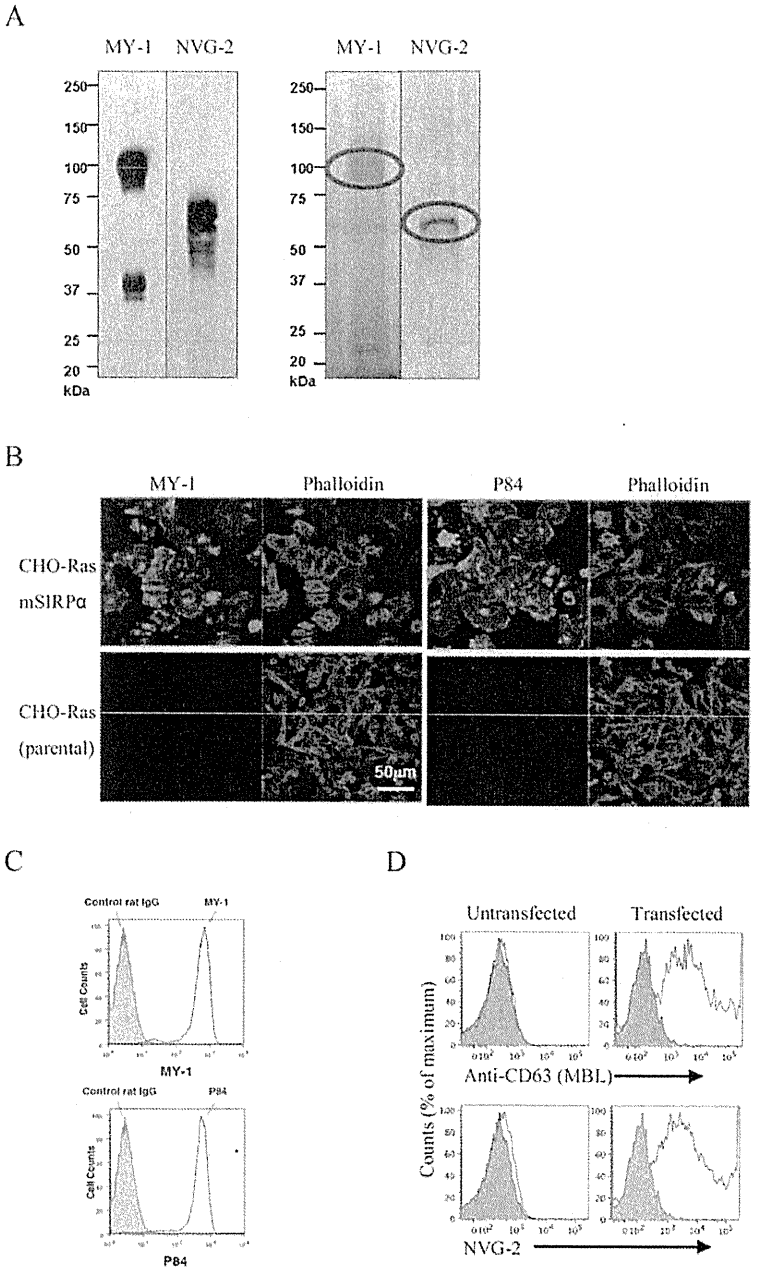

Supplemental Fig. 1. The MY-1 mAb recognizes SIRPα/CD172a, whereas the NVG-2 mAb recognizes a tetraspanin CD63. A. Left panels: Western blot analysis of total cell lysates derived from small intestinal lamina propria with the mAbs MY-1 and NVG-2. Right panels: Silver staining of the materials immunoprecipitated with MY-1 or NVG-2 (major immunoreactive products are indicated by red circles). **B.** The MY-1 mAb binds to SIRPα/CD172a. CHO-Ras cells stably expressing mouse SIRPα/CD172a and the parental cells were fixed and stained with unlabeled MY-1 or P84 mAb (a commercial anti-SIRPα/CD172a). Subsequently, Alexa 488-conjugated anti-rat IgG secondary antibody or Rhodamine-phalloidin was added, and the cells were analyzed by fluorescence microscopy. **C.** Flow cytometry of the CHO-Ras cells stably expressing mouse SIRPα/CD172a. Cells were stained with unlabeled MY-1, P84, or rat IgG2a isotype control antibody (shaded histograms) followed by PE-conjugated anti-rat IgG. The mean fluorescent intensity (MFI) for MY-1 and P84 was 644 and 536, respectively. **D.** The NVG-2 mAb binds to CD63. Flow cytometry of the COS-7 cells expressing mouse CD63 antigen on the cell surface. Transfected and control (untransfected) COS-7 cells were stained with unlabeled anti-CD63 (MBL) or NVG-2 mAb followed by FITC-conjugated goat anti-rat IgG or rat IgG isotype control antibody (shaded histograms).

CD47–signal regulatory protein-α (SIRPα) interactions form a barrier for antibody-mediated tumor cell destruction

Xi Wen Zhao[a], Ellen M. van Beek[a], Karin Schornagel[a], Hans Van der Maaden[b], Michel Van Houdt[a], Marielle A. Otten[c], Pascal Finetti[d], Marjolein Van Egmond[e], Takashi Matozaki[f], Georg Kraal[e], Daniel Birnbaum[d], Andrea van Elsas[b], Taco W. Kuijpers[a,g], Francois Bertucci[d], and Timo K. van den Berg[a,1]

[a]Sanquin Research and Landsteiner Laboratory, Academic Medical Center, University of Amsterdam, 1066 CX Amsterdam, The Netherlands; [b]Departments of Immunotherapeutics and Molecular Pharmacology, Merck Sharp and Dohme Research, 5342 CC, Oss, The Netherlands; [c]Immunotherapy Laboratory, Department of Immunology, University Medical Center, 3584 CX, Utrecht, The Netherlands; [d]Department of Molecular Oncology, Centre de Recherche en Cancérologie de Marseille, Institut Paoli-Calmettes, 13009 Marseille, France; [e]Department of Molecular Cell Biology and Immunology, Vrije University Medical Center, 1081 BT, Amsterdam, The Netherlands; [f]Laboratory of Biosignal Sciences, Institute for Molecular and Cellular Regulation, Gunma University, Gunma 371-8512, Japan; and [g]Emma Children's Hospital, Academic Medical Center, University of Amsterdam, 1105 AZ, Amsterdam, The Netherlands

Edited by Peter K. Vogt, The Scripps Research Institute, La Jolla, CA, and approved October 4, 2011 (received for review April 26, 2011)

Monoclonal antibodies are among the most promising therapeutic agents for treating cancer. Therapeutic cancer antibodies bind to tumor cells, turning them into targets for immune-mediated destruction. We show here that this antibody-mediated killing of tumor cells is limited by a mechanism involving the interaction between tumor cell-expressed CD47 and the inhibitory receptor signal regulatory protein-α (SIRPα) on myeloid cells. Mice that lack the SIRPα cytoplasmic tail, and hence its inhibitory signaling, display increased antibody-mediated elimination of melanoma cells in vivo. Moreover, interference with CD47–SIRPα interactions by CD47 knockdown or by antagonistic antibodies against CD47 or SIRPα significantly enhances the in vitro killing of trastuzumab-opsonized Her2/Neu-positive breast cancer cells by phagocytes. Finally, the response to trastuzumab therapy in breast cancer patients appears correlated to cancer cell CD47 expression. These findings demonstrate that CD47–SIRPα interactions participate in a homeostatic mechanism that restricts antibody-mediated killing of tumor cells. This provides a rational basis for targeting CD47–SIRPα interactions, using for instance the antagonistic antibodies against human SIRPα described herein, to potentiate the clinical effects of cancer therapeutic antibodies.

antibody-dependent cellular cytotoxicity | neutrophil | immunoreceptor | Fc-receptor

Therapeutic monoclonal antibodies (mAbs) directed against tumor cells have become a valuable alternative or addition to conventional cancer treatment modalities. However, despite the beneficial effects documented for various therapeutic antibodies against different types of cancer, antibodies alone are not curative and methods to improve their efficacy are warranted. Therapeutic cancer antibodies may act by one or more several mechanisms, including immune-mediated effects, such as antibody-dependent cellular cytotoxicity (ADCC) and complement-dependent cytotoxicity (CDC) mechanisms, as well as by direct growth-inhibitory effects on tumor cells (1–3).

Currently, the most widely used examples of therapeutic antibodies are rituximab and trastuzumab. Trastuzumab (Herceptin) is a humanized IgG_1 monoclonal antibody approved for the treatment of Her2/Neu-positive breast cancer. Although it is known that trastuzumab binds to the extracellular domain of Her2/Neu, the mechanism(s) of action in patients is not exactly clear. In vitro and in vivo studies in mice suggest that trastuzumab acts by inducing direct G1 growth arrest in breast cancer cells as well as by mediating ADCC (4–6). ADCC can be mediated by Fc receptor-expressing natural killer (NK) cells and phagocytes, including macrophages and granulocytes (7, 8), and a link between FcγRIIa (CD32a) and FcγRIIIa (CD16) polymorphisms and clinical trastuzumab responsiveness in patients with breast cancer suggests an involvement of both types of Fc receptors expressed on phagocytes and NK cells, respectively (3, 9).

NK cell-mediated ADCC is controlled by interactions between "self" MHC class I molecules on (malignant) host cells and inhibitory killer immune receptors (KIRs) expressed on NK cells. Upon ligand binding, inhibitory KIRs recruit and activate the cytosolic tyrosine phosphatases SHP-1 and/or SHP-2 that limit Fc-receptor signaling and, consequently, ADCC toward host cells (7). An inhibitory receptor on myeloid cells, including macrophages and granulocytes, that may potentially act in a similar fashion to restrict antibody-mediated tumor cell elimination is signal regulatory protein (SIRP)α (10–14). The extracellular region of SIRPα interacts with the broadly expressed surface molecule CD47 (15–17). CD47 binding to SIRPα triggers the recruitment and activation of SHP-1 and SHP-2 to immunoreceptor tyrosine-based inhibitory motifs (ITIMs) within the SIRPα cytoplasmic region, and this regulates intracellular signaling pathways and associated downstream functions, usually in a negative fashion (10, 11, 18). It is well-documented, for instance, that SIRPα acts to inhibit in the phagocytosis and in vivo clearance of CD47-expressing host cells, including red blood cells and platelets, by macrophages (19–24). CD47–SIRPα interactions also appear essential for engraftment upon hematopoietic stem cells (25). Based on this, it has been proposed that the broadly expressed CD47 functions, in analogy to MHC class I molecules, as a self signal to control immune effector functions of myeloid cells (19, 26).

Chao et al. (27) have recently reported that antibodies against CD47 synergize with the therapeutic cancer antibody rituximab in the phagocytosis of non-Hodgkin lymphoma by macrophages in immunodeficient mice. However, this study does not provide conclusive evidence for the role of CD47–SIRPα interactions in the context of antibody therapy against cancer. In the present study, we demonstrate that CD47–SIRPα interactions and SIRPα signaling negatively regulate trastuzumab-mediated ADCC in vitro and antibody-dependent elimination of tumor cells in vivo. These findings support the idea that CD47–SIRPα interactions create a barrier for antibody-mediated tumor cell elimination and provide a rational basis for targeting CD47–SIRPα interactions to potentiate the clinical effects of cancer therapeutic antibodies.

Author contributions: M.V.E., G.K., D.B., A.v.E., T.W.K., F.B., and T.K.v.d.B. designed research; X.W.Z., E.M.v.B., K.S., H.V.d.M., M.V.H., and P.F. performed research; M.A.O. and T.M. contributed new reagents/analytic tools; X.W.Z., E.M.v.B., M.V.E., F.B., and T.K.v.d.B. analyzed data; and T.K.v.d.B. wrote the paper.

The authors declare no conflict of interest.

This article is a PNAS Direct Submission.

[1]To whom correspondence should be addressed. E-mail: t.k.vandenberg@sanquin.nl.

This article contains supporting information online at www.pnas.org/lookup/suppl/doi:10.1073/pnas.1106550108/-/DCSupplemental.

Results

Antibody-Mediated Cancer Elimination in Vivo Is Restricted by SIRPα Signaling. We postulated that interactions between CD47, expressed broadly on normal and tumor cells, and the myeloid inhibitory immunoreceptor SIRPα would negatively regulate phagocyte-mediated ADCC induced by cancer therapeutic antibodies, and that targeting of CD47–SIRPα interactions would comprise a generic strategy to improve antibody therapy against cancer. In line with this, Chao et al. (27) have recently shown that antibodies against human CD47 synergize with rituximab in the elimination of non-Hodgkin lymphoma cells in immunodeficient mice and in in vitro phagocytosis experiments. Instead, we used mutant mice lacking the SIRPα cytoplasmic tail (21) to investigate whether inhibitory signaling via SIRPα could regulate the antibody-mediated elimination of syngeneic tumor cells in immunocompetent mice. In particular, we used the well-established mouse metastatic B16 melanoma model, in which the therapeutic antibody TA99, directed against the melanoma gp75 tumor antigen, has shown prominent beneficial effects in tumor cell clearance (28). First, B16F10 cells that expressed surface CD47 (Fig. 1*A*) were injected i.v., in the absence of therapeutic TA99 antibody, into wild-type and SIRPα-mutant mice, and this resulted in a similar tumor formation in both strains of mice (Fig. 1*B*), indicating that SIRPα signaling did not affect tumor cell metastasis and outgrowth per se. Next, these experiments were performed in mice that were treated with suboptimal concentrations of TA99 antibody. TA99 antibody treatment resulted only in a minimal reduction in tumor cell outgrowth in wild-type mice, but tumor formation was essentially abrogated in SIRPα-mutant animals under these conditions (Fig. 1*C*). This demonstrated directly that SIRPα-derived signals can form a limitation for antibody-dependent tumor cell elimination in vivo.

Expression of CD47 in Breast Cancer Correlates with Adverse Features and Resistance to Trastuzumab. In line with the above, we hypothesized that CD47–SIRPα interactions were restricting the clinical efficacy of trastuzumab in the treatment of patients with Her2/Neu-positive breast cancer. To test this hypothesis, we explored a possible relationship between CD47 expression and breast cancer pathological features and clinical trastuzumab responsiveness. To do so, we analyzed breast cancer tissue *CD47* mRNA expression in our cohort of 353 breast cancer patients as well as in a public data set (29). *CD47* mRNA was overexpressed in many tumors, and expression correlated with poor-prognosis molecular subtypes (i.e., basal, Her2/Neu$^+$) (Fig. 2*A*) and with adverse pathological features [i.e., high-grade, estrogen receptor (ER)$^-$, progesterone receptor (PR)$^-$]. Furthermore, analysis of a relatively small public data set (29) of Her2/Neu-positive breast cancer patients treated with trastuzumab plus vinorelbine revealed an inverse correlation between *CD47* expression level and pathological response to the therapy (Fig. 2*B*), with significantly lower *CD47* expression in complete responders. Although the latter finding clearly requires confirmation in a larger and independent patient cohort, it is consistent with an adverse role of CD47 in the trastuzumab-mediated elimination of breast cancer cells.

Targeting CD47–SIRPα Interactions Potentiates Trastuzumab-Mediated ADCC Against Breast Cancer Cells. To directly investigate whether CD47–SIRPα interactions play a role in the trastuzumab-dependent destruction of breast cancer cells by phagocytes, we established an in vitro ADCC assay using trastuzumab-opsonized human SKBR-3 breast cancer cells expressing surface Her2/Neu and CD47 (Fig. 3*A*) as targets and human neutrophils as effector cells. Trastuzumab-mediated ADCC by neutrophils was potently and synergistically enhanced by F(ab′)$_2$ fragments of the B6H12 mAb that blocks CD47 binding to SIRPα (30) (Fig. 3 *B–E*). The enhancing effect of blocking anti-CD47 F(ab′)$_2$ was observed at different effector:target (E:T) ratios (Fig. 3*C*) and appeared to act by both decreasing the threshold as well as by increasing the magnitude of killing (Fig. 3*D*). Importantly, in the absence of trastuzumab, no detectable tumor killing effect of anti-CD47 F(ab′)$_2$ was observed, suggesting that CD47–SIRPα interactions do not control antibody-independent mechanisms of killing. This observation is in apparent contrast with the results of Chao et al. (27, 31), who also reported significant effects on lymphoma phagocytosis with the anti-CD47 mAb B6H12 alone. The latter may possibly relate, at least in part, to their use of intact B6H12 mAb that according to our own results can indeed cause direct ADCC in SKBR-3 cells (Fig. S1).

In the numerous independent experiments ($n > 50$) that were performed with neutrophils as effector cells for killing of tras-

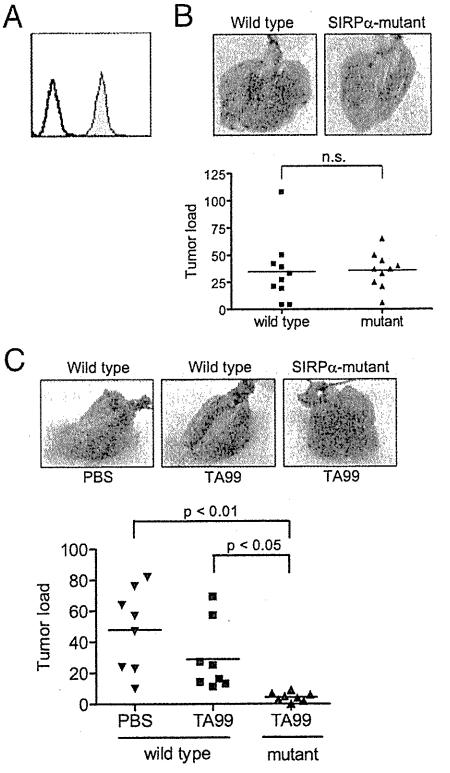

Fig. 1. SIRPα signaling limits antibody-mediated destruction of melanoma cells in vivo. (*A*) CD47 expression on B16F10 mouse melanoma cells as demonstrated by flow cytometry using anti-mouse CD47 antibody (Miap301) and phycoerythrin-labeled anti-mouse IgG (filled histogram). The open histogram represents the isotype control. (*B*) Comparable outgrowth of B16 melanoma in wild-type and SIRPα-mutant mice in the absence of therapeutic antibody. Wild-type and SIRPα-mutant mice were injected i.v. with 1.5×10^5 B16F10 tumor cells. After 21 d, mice were killed, lungs were excised and photographed (representative examples are shown), and tumor loads were determined and expressed as the sum of the following scores: metastases less than 1 mm were scored as 1; metastases between 1 and 2 mm were scored as 3; and metastases larger than 2 mm were scored as 10. Measurements from individual mice are shown, with means indicated by bars, and statistical differences between groups (n = 10) were determined by ANOVA. Note that comparable tumor loads occur in wild-type (34.7 ± 9.5) (mean ± SEM) and SIRPα-mutant mice (35.9 ± 5.2). Data are from one representative experiment out of three. (*C*) Enhanced antibody-mediated clearance of B16 melanoma cells in SIRPα-mutant mice. Wild-type and SIRPα-mutant mice were challenged i.v. with 1.5×10^5 B16F10 tumor cells and, where indicated, with a suboptimal dose of 10 μg of TA99 antibody (or PBS as control) on days 0, 2, and 4. After 21 d, mice were killed and analyzed as in *B*. Measurements from individual mice are shown, with means indicated by bars, and statistical differences between groups (n = 8) were determined by ANOVA. Note the black nodules of melanoma lung metastases in *B* and *C*. Note in the graph in *C* that TA99 antibody treatment resulted only in a minimal nonsignificant reduction in tumor cell outgrowth in wild-type animals [47.9 ± 9.4 (mean ± SEM) in PBS-treated mice compared with 29.0 ± 7.8 in TA99-treated mice], but tumor formation was essentially absent in SIRPα-mutant animals treated with TA99 antibody (4.5 ± 1.0). Data are from one representative experiment out of three.

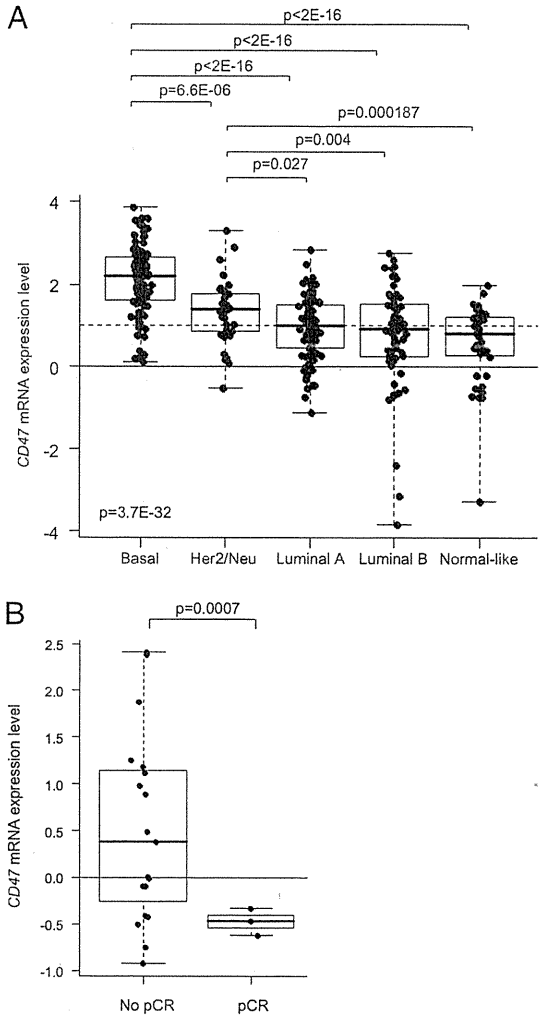

Fig. 2. *CD47* mRNA expression in breast cancer. (*A*) Correlation with molecular subtypes: basal, Her2/Neu-positive, luminal A, luminal B, and normal-like (Institut Paoli-Calmettes series; n = 353). Log_2-transformed expression levels in tumors are reported as box plots relative to expression in normal breast (NB; horizontal solid line). Overexpression (ratio T:NB ≥2; horizontal dashed line) of CD47 was found in 63% of tumors. Note that the poor-prognosis subtypes (i.e., basal and Her2/Neu$^+$) have the highest *CD47* expression levels. Differences in expression levels between the five subtypes were tested for significance using one-way ANOVA, and between two subtypes using Student's t test. (*B*) Correlation with pathological response to trastuzumab plus vinorelbine treatment [public data set (29); n = 22]. Log_2-transformed expression levels in tumors are reported as box plots relative to median expression in all samples (median; horizontal solid line). Note that patients with a pathological complete response (pCR; n = 3) have significantly lower *CD47* expression than patients with an incomplete response (no pCR; n = 19).

tuzumab-opsonized SKBR-3 cells a consistent enhancing effect of anti-CD47 $F(ab')_2$ was observed, although the degree of killing (with trastuzumab alone) varied considerably for different effector cell donors (Fig. 3*B*). The latter appeared to be related to a factor(s) intrinsic to the effector cells, including individual differences in the expression of FcγRI and FcγRIIIb receptors that is pivotal for the induction of ADCC (Fig. S2).

Reduction of CD47 in Breast Cancer Cells Promotes Trastuzumab-Mediated ADCC. To further study a regulatory role of CD47–SIRPα interactions in ADCC, siRNA-mediated knockdown of CD47 expression was performed in SKBR-3 target cells. This yielded cells with 80–90% reduced surface CD47 expression (Fig. 4*A*). These cells were significantly more sensitive toward neutrophil-mediated ADCC, consistent with a role for CD47–SIRPα interactions in restricting tumor cell killing (Fig. 4*B*). The increase was comparable to levels seen with wild-type SKBR-3 cells in the presence of blocking anti-CD47 $F(ab')_2$.

Unique mAb Against SIRPα Potentiates Trastuzumab-Mediated ADCC Against Breast Cancer Cells. Although the above strongly supported the idea that CD47–SIRPα interactions regulate ADCC in vitro and tumor elimination in vivo, it was important to confirm these findings with blocking antibodies against SIRPα. In fact, because of its much more restricted expression (12, 16), we anticipate that SIRPα, rather than the ubiquitous CD47, constitutes the preferred target for potential future therapeutic intervention. Because the previously reported antibodies against human SIRPα available to us either lacked the proper specificity or the ability to block interactions with CD47, we generated unique blocking mAbs against $SIRP\alpha_1$. One antibody, designated 1.23A, was generated by electrofusion technology following negative selection on CHO cells expressing the myeloid-specific SIRP family member $SIRP\beta_1$, whereas the other, designated 12C4, was generated by conventional hybridoma technology. Both of the two SIRPα polymorphic variants predominating in the Caucasian population, $SIRP\alpha_1$ and $SIRP\alpha_{BIT}$, as well as the highly homologous myeloid $SIRP\beta_1$ and nonmyeloid SIRPγ family members were recognized by 12C4, but the 1.23A mAb exclusively recognized the $SIRP\alpha_1$ variant (Fig. S3 *A* and *B*). Staining of leukocytes from SIRPα-genotyped individuals was consistent with this specificity (Fig. S3*C*), with the mAb 1.23A selectively recognizing monocytes and neutrophils from both α_1/α_1-homozygous and α_1/α_{BIT}-heterozygous individuals. Both mAbs effectively inhibited the binding of CD47-coated beads to CHO cells expressing $SIRP\alpha_1$ and/or $SIRP\alpha_{BIT}$ (Fig. 5*A*) and promoted trastuzumab-mediated ADCC toward SKBR-3 cells by neutrophils from individuals with different genotypes (Fig. 5 *B* and *C*). For the 1.23A mAb, enhanced killing was only observed when neutrophils from α_1/α_1-homozygous individuals were used. When $\alpha_{BIT}/\alpha_{BIT}$-homozygous or α_1/α_{BIT}-heterozygous donor cells were used, 1.23A did not enhance SKBR-3 killing by trastuzumab, suggesting that the presence of a single functional allele of SIRPα is sufficient to restrict ADCC and that both alleles have to be inhibited simultaneously to achieve a beneficial effect accordingly.

Discussion

In the present study, we have investigated the role of CD47–SIRPα interactions in the context of antibody therapy against cancer. In general, our results provide evidence that CD47–SIRPα interactions, and the resultant intracellular signals generated via SIRPα in myeloid cells, suppress antibody-mediated destruction of tumor cells.

To study the role of SIRPα in vivo, we used mutant mice lacking the SIRPα cytoplasmic tail to investigate whether inhibitory signaling via SIRPα could regulate the antibody-mediated elimination of syngeneic B16F10 melanoma cells in immunocompetent mice. Our results demonstrate that SIRPα signaling does indeed limit the capacity of cancer therapeutic antibodies to eliminate tumor cells in vivo. The effects could not be attributed to direct effects of SIRPα on tumor homing or outgrowth, as identical tumor development was shown in the absence of therapeutic antibody. This provides evidence for a role of SIRPα in antibody-mediated tumor cell destruction in vivo.

The role of CD47–SIRPα interactions in a human context was investigated with an in vitro ADCC method using trastuzumab-opsonized Her2/Neu-positive SKBR-3 breast cancer cells as target cells and neutrophils as effector cells. In this assay, the addition of $F(ab')_2$ fragments of the antibody B6H12, which is known to block CD47–SIRPα interactions (30), substantially enhanced trastuzumab-mediated cancer cell killing, supporting the idea that CD47–SIRPα interactions negatively control ADCC. Of note, the interference with CD47–SIRPα interactions in the absence of tras-

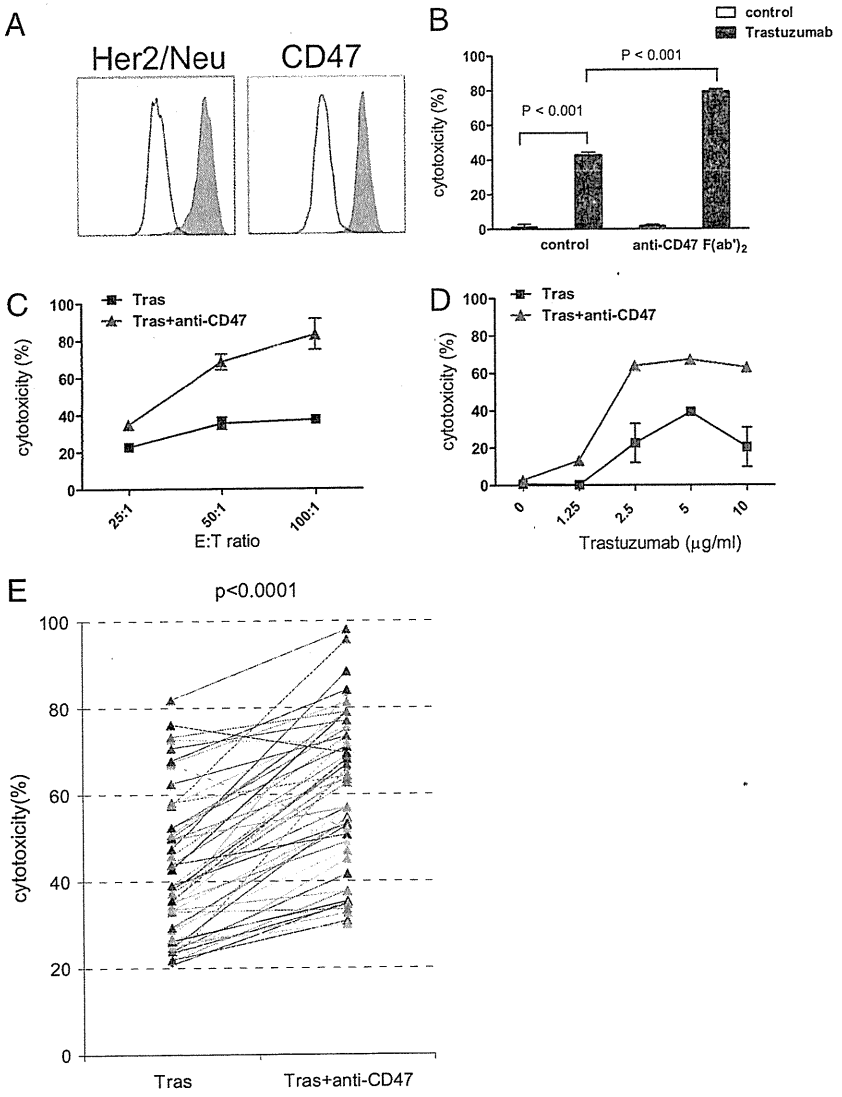

Fig. 3. Interference with CD47–SIRPα interactions using blocking anti-CD47 antibody B6H12 potentiates trastuzumab-mediated ADCC of neutrophils toward Her2/Neu-positive SKBR-3 breast cancer cells. (*A*) Flow cytometric analysis of Her2/Neu and CD47 surface expression on SKBR-3 breast cancer cells (filled histograms), using trastuzumab and B6H12 mAb, respectively, against CD47. Isotype controls are shown in the open histograms. (*B*) ADCC of neutrophils against trastuzumab-opsonized SKBR-3 cells (E:T ratio, 50:1) in the absence or presence of B6H12 anti-CD47 F(ab')$_2$. Shown is a representative example. Results are expressed as means ± SD of triplicate measurements, and statistical differences were shown by Student's *t* test. Note that anti-CD47 F(ab')$_2$ fragments do not affect cytotoxicity alone, but do synergize with trastuzumab. (*C* and *D*) Blocking CD47–SIRPα interactions using anti-CD47 F(ab')$_2$ enhances the ADCC of neutrophils against trastuzumab-opsonized SKBR-3 cells at different E:T ratios (*C*) and trastuzumab concentrations (*D*). Shown is a representative experiment out of three. (*E*) The effects of anti-CD47 F(ab')$_2$ on ADCC toward trastuzumab-opsonized SKBR-3 cells using neutrophils from different donors in multiple independent experiments ($n = 53$). For clarity, only the values in the presence of trastuzumab ± anti-CD47 F(ab')$_2$ are shown, with the matched values of the two conditions for each donor connected by lines. Killing in the absence of trastuzumab ± anti-CD47 F(ab')$_2$ was always below 5%. *P* values of statistically significant differences, as determined by Student's *t* test, are indicated.

tuzumab did not enhance ADCC. The latter is in apparent contrast with the results of Chao et al., who did show significant effects of anti-CD47 antibody alone on tumor cell phagocytosis in vitro and in vivo. However, Chao et al. used intact B6H12 anti-CD47 antibody in the vast majority of their experiments, including all of their in vivo experiments. We now demonstrate that this intact anti-CD47 antibody causes direct ADCC in neutrophils (Fig. S1), and similar observations have also been made for monocytes/macrophages, thereby indicating, in retrospect, that the results of Chao et al. did not really justify the conclusion that the effects were due to the interference with CD47–SIRPα interactions. On the contrary, our findings, which are based on both antibody-blocking experiments performed with anti-CD47 F(ab')$_2$ fragments as well as CD47 knockdowns in breast cancer cells, do indeed exclude alternative explanations and thereby provide direct evidence for a regulatory role of CD47–SIRPα interactions in antibody-dependent cancer cell destruction.

Although the above clearly supported a role for CD47–SIRPα interactions in antibody-dependent tumor cell elimination, it was considered important to confirm these results with antagonistic antibodies against SIRPα. Moreover, because of its much more limited tissue distribution compared with CD47, SIRPα appears to be the preferred target for potential future therapeutic intervention. Because antagonistic antibodies of the appropriate specificity were unavailable, we attempted to generate new reagents. Two antagonistic antibodies were identified and characterized that reacted with one or both of the two major [and apparently equally functional (32)] polymorphic SIRPα variants, SIRPα$_1$ and SIRPα$_{BIT}$, found in the Caucasian population, and both were shown to be able to enhance trastuzumab-mediated ADCC in breast cancer cells. Notably, the inability of the SIRPα$_1$-specific antibody to enhance antibody-dependent tumor cell elimination when effector cells from heterozygote SIRPα$_1$/SIRPα$_{BIT}$ individuals were used suggests that inhibitory signals from both alleles are required to provide substantial control over antibody-mediated cytotoxicity. It will be of interest to test the in vivo efficacy of our antibodies in appropriately humanized mouse xenograft tumor models.

Clearly, an interesting and clinically highly relevant question is whether CD47–SIRPα interactions play a regulatory role in the context of antibody therapy in human cancer patients, and whether antagonists targeting the CD47–SIRPα interaction, such as the antibodies against SIRPα described herein, can be used to enhance the clinical efficacy of trastuzumab. Although the present study does not provide direct evidence for this, our findings do suggest a preliminary link between CD47 expression on breast cancer cells and clinical trastuzumab responsiveness in breast cancer. In particular, pathologically complete responders were found to have

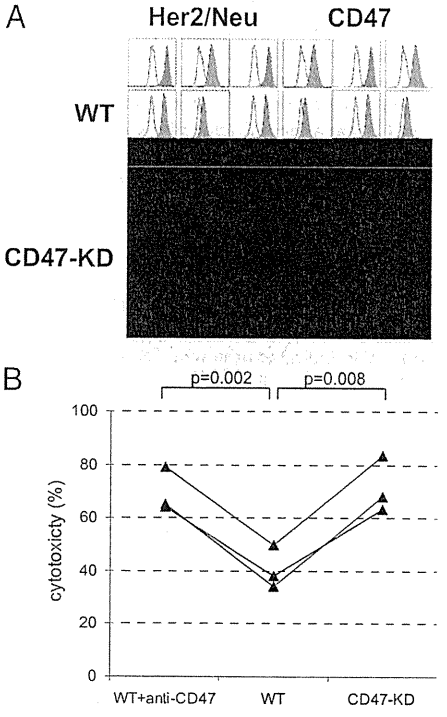

Fig. 4. Knockdown of CD47 in SKBR-3 breast cancer target cells enhances trastuzumab-dependent neutrophil-mediated ADCC. (*A*) Flow cytometric analysis for Her2/Neu and CD47 surface expression in SKBR-3 cells transfected with empty vector (control) or *CD47* shRNA (CD47-KD). Note that CD47 expression is strongly decreased in the CD47-KD cells (mean fluorescence intensity (MFI) = 358 in CD47-KD cells vs. MFI = 4.187 in control), but Her2/Neu levels are unaltered (MFI = 18.638 in CD47-KD cells and MFI = 18.993 in control). (*B*) Neutrophil-mediated ADCC using control and CD47-KD SKBR-3 cells opsonized with trastuzumab in three independent experiments with three different effector cell donors. Note that a similar level of enhancement occurs with anti-CD47 $F(ab')_2$-mediated blocking and CD47 knockdown. *P* values of statistically significant differences, as determined by Student's *t* test, are indicated.

significantly lower CD47 mRNA levels compared with trastuzumab-treated patients lacking a pathologically complete response.

It should be emphasized that CD47–SIRPα interactions may not form the only mechanism by which tumor cells can evade phagocyte-mediated immune destruction. In fact, recent studies have shown that the interaction between the self CD200 molecule, expressed on tumor cells and many other cell types, and the nonconventional (i.e., ITIM-lacking) inhibitory CD200 receptor (CD200R) on myeloid cells may also limit the immune-mediated elimination of leukemic cells such as B-CLL (33–35). However, this can apparently occur in the absence of therapeutic antibodies, and may also be mediated by a different effector mechanism involving cytotoxic T cells. The observation that different nonredundant mechanisms may actually underlie the regulatory effects of the CD47–SIRPα and CD200–CD200R interactions may actually generate opportunities for simultaneous targeting of these pathways to increase therapeutic benefit.

Collectively, our results provide direct evidence for a homeostatic regulatory role of CD47–SIRPα interactions in the context of antibody-mediated destruction of tumor cells by myeloid cells. Together with the findings of Chao et al. (27), this provides a strong rational basis for combining therapeutic antibodies against cancer cells with antagonists of the CD47–SIRPα interaction, such as the mAb against SIRPα described here. This is anticipated to enhance the clinical efficacy of cancer-targeting therapeutic antibodies and/or reduce the need for chemotherapy or other nonspecific treatment regimens.

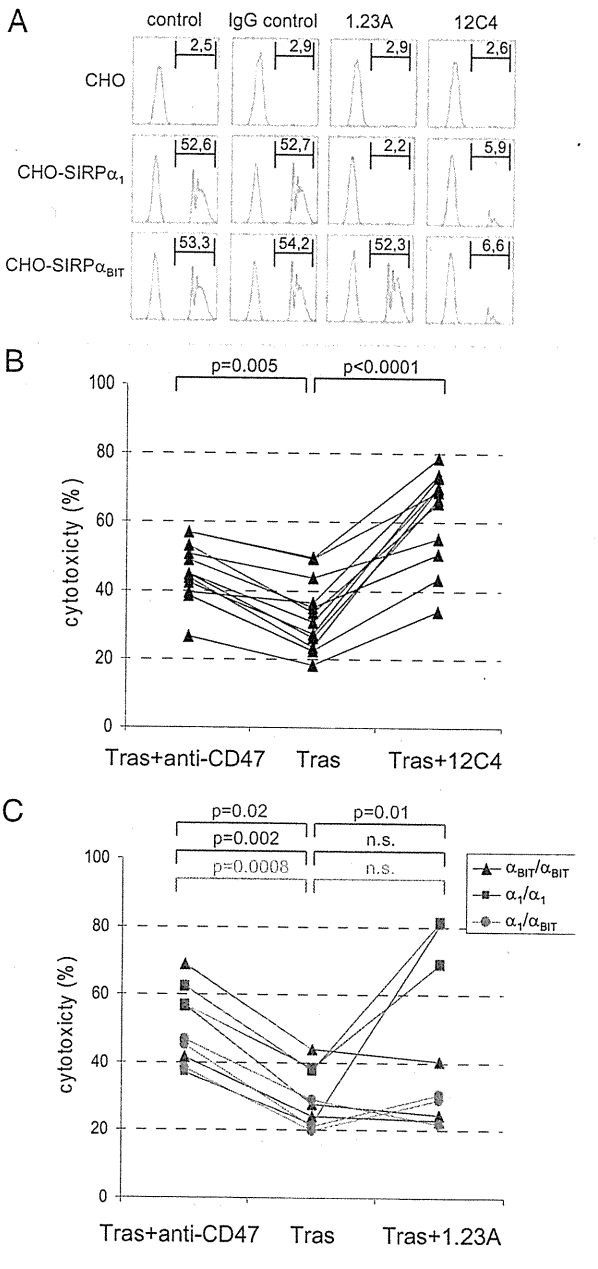

Fig. 5. Monoclonal antibodies against SIRPα that block CD47–SIRPα interactions enhance ADCC. (*A*) CD47-coated fluorescent bead binding to CHO cells expressing empty vector (i.e., "CHO"), $SIRP\alpha_1$, or $SIRP\alpha_{BIT}$. The 12C4 and 1.23A mAbs (but not isotype IgG_1 control mAb) block the binding of CD47 beads to either both $SIRP\alpha_1$- and $SIRP\alpha_{BIT}$-expressing CHO cells (12C4) or only to $SIRP\alpha_1$-expressing CHO cells. The proportion (in %) of cells binding CD47 beads is indicated in the upper right of each panel. Shown is one representative experiment out of three. (*B*) Enhancing effect of 12C4 mAb on ADCC toward trastuzumab-opsonized SKBR-3 cells using neutrophils from ($n = 12$) individuals in four independent experiments. (*C*) Enhancing effect of 1.23A mAb on ADCC toward trastuzumab-opsonized SKBR-3 cells using neutrophils from ($n = 9$) individuals with different SIRPα genotypes (α_1/α_1 or $\alpha_{BIT}/\alpha_{BIT}$ homozygotes or α_1/α_{BIT} heterozygotes) in three independent experiments. *P* values of statistically significant differences, as determined by Student's *t* test, are indicated. n.s., nonsignificant.

Methods

Mice and B16 Melanoma Model. C57BL/6 mice with a targeted deletion of the SIRPα cytoplasmic region have been described previously (21). These mice, originally generated onto the 129/Sv background and backcrossed onto

C57BL/6 mice for 10 generations, were bred and maintained under specific pathogen-free conditions, together with wild-type C57BL/6 mice from the same genetic background, and used between 8 and 12 wk of age. Age-matched wild-type and SIRPα-mutant mice were injected i.v. with 1.5×10^5 B16F10 tumor cells in 100 μL of HBSS on day 0. Mice were injected i.p. with a suboptimal dose of 10 μg of TA99 antibody (or PBS as control) on days 0, 2, and 4. At day 21 the mice were killed. Their lungs were excised and scored for the number of metastases and tumor load as described (28).

Antibodies, cell lines, culture conditions, procedures for the production of monoclonal antibodies, the CD47 bead binding assay, and flow cytometry are described in *SI Methods*.

***CD47* mRNA Expression in Breast Cancer.** We analyzed *CD47* mRNA expression in 353 invasive breast carcinomas and 11 normal breast samples profiled (36) using whole-genome Affymetrix oligonucleotide microarrays (Gene Expression Omnibus accession no. GSE21653). Only two of the probe sets representing *CD47*, 211075_s_at and 213857_s_at, mapped exclusively to constitutively transcribed *CD47* exons according to NetAffx, RefSeq, and the University of California Santa Cruz Genome Browser (27). Their expression strongly correlated (Spearman correlation, 0.87). We retained that with the highest variance (211075_s_at). Before analysis, the *CD47* expression level for each tumor was centered by the average expression level of the normal breast samples. We analyzed the correlation between *CD47* expression and patients' age (≤/>50 y), pathological tumor size (≤/>2 cm), axillary lymph node status (negative/positive) and grading (I/II/III), immunohistochemisty estrogen and progesterone receptor status (negative/positive; positivity threshold 10% of tumor cells), and molecular subtypes (luminal A/luminal B/basal/Her2/Neu$^+$/normal-like), defined as described (37). We also analyzed a public (http://caarraydb.nci.nih.gov/ccarray) expression data set of Her2/Neu-positive breast cancers treated with primary trastuzumab plus vinorelbine weekly for 12 wk followed by surgery (29). Pathological complete response was defined as the absence of invasive cancer in the breast and axillary lymph nodes at the time of surgery.

ADCC Assay. Neutrophils were isolated by density centrifugation from heparinized blood obtained from healthy volunteers using isotonic Percoll (Pharmacia) followed by red cell lysis with hypotonic ammonium chloride solution. Cells were cultured in complete RPMI medium in the presence of 10 ng/mL clinical grade G-CSF (Neupogen; Amgen) and 50 ng/mL recombinant human IFN-γ (PeproTech) at a concentration of 5×10^6 cells/mL for 16–20 h. Monocytes were isolated from the peripheral blood mononuclear cells fraction by magnetic cell sorting using anti-CD14-coated beads according to the manufacturer's instructions (Miltenyi Biotec) or by counterflow elutriation. Washed tumor cells ($5–8 \times 10^6$ cells) were collected and labeled with 100 μCi ^{51}Cr (PerkinElmer) in 1 mL for 90 min at 37 °C. The cells were preincubated with anti-CD47 and/or the therapeutic antibodies, as indicated, and washed again. The target cells (5×10^3 per well) and effector cells were cocultured in 96-well U-bottom tissue culture plates in complete medium in an E:T ratio of 50:1, unless indicated otherwise, for 4 h at 37 °C in 5% CO_2 in RPMI with 10% FCS medium. Aliquots of supernatant were harvested and analyzed for radioactivity in a gamma counter. The percent relative cytotoxicity was determined as [(experimental cpm − spontaneous cpm)/(total cpm − spontaneous cpm)] × 100%. All conditions were measured in triplicate.

Statistical Analysis. Statistical differences were determined using ANOVA or Student's *t* test as indicated.

ACKNOWLEDGMENTS. We thank Dr. L. A. Aarden and Dr. S. Rodenhuis for useful discussions and supplying anti-CD3, rituximab, and trastuzumab antibodies; and Dr. D. Roos and Dr. R. van Lier for their advice on the manuscript. Miap301 and B6H12 antibodies were generously provided by Dr. E. Brown (University of California at San Francisco). Dr. Peter Steenbakkers is acknowledged for his help in generating anti-SIRPα mAb. Paul Verkuijlen and Peter Kooyman are gratefully acknowledged for their technical support.

1. Glennie MJ, van de Winkel JG (2003) Renaissance of cancer therapeutic antibodies. *Drug Discov Today* 8:503–510.
2. Oldham RK, Dillman RO (2008) Monoclonal antibodies in cancer therapy: 25 years of progress. *J Clin Oncol* 26:1774–1777.
3. Strome SE, Sausville EA, Mann D (2007) A mechanistic perspective of monoclonal antibodies in cancer therapy beyond target-related effects. *Oncologist* 12:1084–1095.
4. Clynes RA, Towers TL, Presta LG, Ravetch JV (2000) Inhibitory Fc receptors modulate in vivo cytoxicity against tumor targets. *Nat Med* 6:443–446.
5. Barok M, et al. (2007) Trastuzumab causes antibody-dependent cellular cytotoxicity-mediated growth inhibition of submacroscopic JIMT-1 breast cancer xenografts despite intrinsic drug resistance. *Mol Cancer Ther* 6:2065–2072.
6. Spiridon CI, Guinn S, Vitetta ES (2004) A comparison of the in vitro and in vivo activities of IgG and F(ab')$_2$ fragments of a mixture of three monoclonal anti-Her-2 antibodies. *Clin Cancer Res* 10:3542–3551.
7. Lanier LL (2005) NK cell recognition. *Annu Rev Immunol* 23:225–274.
8. van Spriel AB, van Ojik HH, Bakker A, Jansen MJ, van de Winkel JG (2003) Mac-1 (CD11b/CD18) is crucial for effective Fc receptor-mediated immunity to melanoma. *Blood* 101:253–258.
9. Musolino A, et al. (2008) Immunoglobulin G fragment C receptor polymorphisms and clinical efficacy of trastuzumab-based therapy in patients with HER-2/neu-positive metastatic breast cancer. *J Clin Oncol* 26:1789–1796.
10. Fujioka Y, et al. (1996) A novel membrane glycoprotein, SHPS-1, that binds the SH2-domain-containing protein tyrosine phosphatase SHP-2 in response to mitogens and cell adhesion. *Mol Cell Biol* 16:6887–6899.
11. Kharitonenkov A, et al. (1997) A family of proteins that inhibit signalling through tyrosine kinase receptors. *Nature* 386:181–186.
12. Adams S, et al. (1998) Signal-regulatory protein is selectively expressed by myeloid and neuronal cells. *J Immunol* 161:1853–1859.
13. van Beek EM, Cochrane F, Barclay AN, van den Berg TK (2005) Signal regulatory proteins in the immune system. *J Immunol* 175:7781–7787.
14. Barclay AN, Brown MH (2006) The SIRP family of receptors and immune regulation. *Nat Rev Immunol* 6:457–464.
15. Jiang P, Lagenaur CF, Narayanan V (1999) Integrin-associated protein is a ligand for the P84 neural adhesion molecule. *J Biol Chem* 274:559–562.
16. Seiffert M, et al. (2001) Signal-regulatory protein α (SIRPα) but not SIRPβ is involved in T-cell activation, binds to CD47 with high affinity, and is expressed on immature CD34(+)CD38(−) hematopoietic cells. *Blood* 97:2741–2749.
17. Vernon-Wilson EF, et al. (2000) CD47 is a ligand for rat macrophage membrane signal regulatory protein SIRP (OX41) and human SIRPα 1. *Eur J Immunol* 30:2130–2137.
18. Timms JF, et al. (1998) Identification of major binding proteins and substrates for the SH2-containing protein tyrosine phosphatase SHP-1 in macrophages. *Mol Cell Biol* 18:3838–3850.
19. Oldenborg PA, et al. (2000) Role of CD47 as a marker of self on red blood cells. *Science* 288:2051–2054.
20. Olsson M, Bruhns P, Frazier WA, Ravetch JV, Oldenborg PA (2005) Platelet homeostasis is regulated by platelet expression of CD47 under normal conditions and in passive immune thrombocytopenia. *Blood* 105:3577–3582.
21. Yamao T, et al. (2002) Negative regulation of platelet clearance and of the macrophage phagocytic response by the transmembrane glycoprotein SHPS-1. *J Biol Chem* 277:39833–39839.
22. Ishikawa-Sekigami T, et al. (2006) SHPS-1 promotes the survival of circulating erythrocytes through inhibition of phagocytosis by splenic macrophages. *Blood* 107:341–348.
23. Okazawa H, et al. (2005) Negative regulation of phagocytosis in macrophages by the CD47-SHPS-1 system. *J Immunol* 174:2004–2011.
24. Oldenborg PA, Gresham HD, Lindberg FP (2001) CD47-signal regulatory protein α (SIRPα) regulates Fcγ and complement receptor-mediated phagocytosis. *J Exp Med* 193:855–862.
25. Takenaka K, et al. (2007) Polymorphism in Sirpa modulates engraftment of human hematopoietic stem cells. *Nat Immunol* 8:1313–1323.
26. van den Berg TK, van der Schoot CE (2008) Innate immune 'self' recognition: A role for CD47–SIRPα interactions in hematopoietic stem cell transplantation. *Trends Immunol* 29:203–206.
27. Chao MP, et al. (2010) Anti-CD47 antibody synergizes with rituximab to promote phagocytosis and eradicate non-Hodgkin lymphoma. *Cell* 142:699–713.
28. Hara I, Takechi Y, Houghton AN (1995) Implicating a role for immune recognition of self in tumor rejection: Passive immunization against the brown locus protein. *J Exp Med* 182:1609–1614.
29. Harris LN, et al. (2007) Predictors of resistance to preoperative trastuzumab and vinorelbine for HER2-positive early breast cancer. *Clin Cancer Res* 13:1198–1207.
30. Latour S, et al. (2001) Bidirectional negative regulation of human T and dendritic cells by CD47 and its cognate receptor signal-regulator protein-α: Down-regulation of IL-12 responsiveness and inhibition of dendritic cell activation. *J Immunol* 167:2547–2554.
31. Chao MP, et al. (2011) Therapeutic antibody targeting of CD47 eliminates human acute lymphoblastic leukemia. *Cancer Res* 71:1374–1384.
32. Hatherley D, Graham SC, Harlos K, Stuart DI, Barclay AN (2009) Structure of signal-regulatory protein α: A link to antigen receptor evolution. *J Biol Chem* 284:26613–26619.
33. McWhirter JR, et al. (2006) Antibodies selected from combinatorial libraries block a tumor antigen that plays a key role in immunomodulation. *Proc Natl Acad Sci USA* 103:1041–1046.
34. Kretz-Rommel A, et al. (2007) CD200 expression on tumor cells suppresses antitumor immunity: New approaches to cancer immunotherapy. *J Immunol* 178:5595–5605.
35. Kretz-Rommel A, et al. (2008) Blockade of CD200 in the presence or absence of antibody effector function: Implications for anti-CD200 therapy. *J Immunol* 180:699–705.
36. Bertucci F, et al. (2006) Gene expression profiling shows medullary breast cancer is a subgroup of basal breast cancers. *Cancer Res* 66:4636–4644.
37. Sabatier R, et al. (2011) A gene expression signature identifies two prognostic subgroups of basal breast cancer. *Breast Cancer Res Treat* 126:407–420.

Signal Regulatory Protein α Regulates the Homeostasis of T Lymphocytes in the Spleen

Miho Sato-Hashimoto,* Yasuyuki Saito,*,† Hiroshi Ohnishi,* Hiroko Iwamura,* Yoshitake Kanazawa,* Tetsuya Kaneko,* Shinya Kusakari,* Takenori Kotani,* Munemasa Mori,* Yoji Murata,‡ Hideki Okazawa,‡ Carl F. Ware,§ Per-Arne Oldenborg,¶ Yoshihisa Nojima,† and Takashi Matozaki*,‡

The molecular basis for formation of lymphoid follicle and its homeostasis in the secondary lymphoid organs remains unclear. Signal regulatory protein α (SIRPα), an Ig superfamily protein that is predominantly expressed in dendritic cells or macrophages, mediates cell–cell signaling by interacting with CD47, another Ig superfamily protein. In this study, we show that the size of the T cell zone as well as the number of $CD4^+$ T cells were markedly reduced in the spleen of mice bearing a mutant (MT) SIRPα that lacks the cytoplasmic region compared with those of wild-type mice. In addition, the expression of CCL19 and CCL21, as well as of IL-7, which are thought to be important for development or homeostasis of the T cell zone, was markedly decreased in the spleen of SIRPα MT mice. By the use of bone marrow chimera, we found that hematopoietic SIRPα is important for development of the T cell zone as well as the expression of CCL19 and CCL21 in the spleen. The expression of lymphotoxin and its receptor, lymphotoxin β receptor, as well as the in vivo response to lymphotoxin β receptor stimulation were also decreased in the spleen of SIRPα MT mice. CD47-deficient mice also manifested phenotypes similar to SIRPα MT mice. These data suggest that SIRPα as well as its ligand CD47 are thus essential for steady-state homeostasis of T cells in the spleen. *The Journal of Immunology*, **2011, 187: 291–297.**

Secondary lymphoid organs, spleen and lymph nodes (LN), are sites for induction of primary immune responses that provide critical microenvironments to facilitate interactions between cells of the innate and adaptive immune systems (1). In mouse spleen, the splenic white pulp consists of T cells zones surrounding a central arteriole, as well as B cell follicles and their surrounding marginal zones (1, 2). The positioning and segregation of T and B lymphocytes into their compartments in the white pulp in the spleen are controlled by homeostatic chemokines, including CCL19, CCL21, and CXCL13. CCL19 and CCL21 are thought to attract naive T cells that express CCR7, a receptor for CCL19 or CCL21, into periarterial lymphoid sheathes (PALS) in the spleen (1, 3). By contrast, CXCL13 is thought to attract B cells, which express a CXCL13 receptor, CXCR5, into lymphoid follicles (1, 2, 4). Both CCL19 and CCL21 are produced by stromal cells in the PALS of spleen, named fibroblastic reticular cells (FRCs), whereas CXCL13 is produced by stromal cells present in the B cell follicles of the spleen (1, 3, 5). IL-7, which is also produced by FRCs in the T cell zone of the spleen, is thought to be a major cytokine that maintains the homeostasis of T cells, particularly naive T cells, by promoting their survival and proliferation (6).

In addition to these chemokines or cytokines, membrane-bound molecules are also thought to be important for homeostatic regulation of T cells. Indeed, interaction of self-Ag–presenting MHC molecules of dendritic cells (DCs) with TCR promotes the survival of naive T cells by activation of TCR signaling (6–9). Lymphotoxin (LT) $\alpha_1\beta_2$, a membrane-anchored heterotrimer expressed in B and T cells, interacts with the LTβ receptor (LTβR) expressed on FRCs and is essential for production of homeostatic chemokines, CCL19 or CCL21, by FRCs (2, 10, 11). However, the molecular basis for regulation of T cell homeostasis in the spleen by membrane-bound molecules remains largely uncharacterized.

Signal regulatory protein α (SIRPα), also known as Src homology 2 domain-containing protein tyrosine phosphatase (SHP) substrate-1 or brain Ig-like molecule with tyrosine-based activation motifs (12, 13), is a transmembrane protein in which the extracellular region comprises three Ig-like domains and the cytoplasmic region contains ITIM that mediate binding of the protein tyrosine phosphatases SHP-1 and SHP-2. Tyrosine phosphorylation of SIRPα is triggered by various growth factors and cytokines as well as by integrin-mediated cell adhesion to extracellular

*Laboratory of Biosignal Sciences, Institute for Molecular and Cellular Regulation, Gunma University, Gunma 371-8512, Japan; †Department of Medicine and Clinical Science, Gunma University Graduate School of Medicine, Gunma 371-8511, Japan; ‡Division of Molecular and Cellular Signaling, Department of Biochemistry and Molecular Biology, Kobe University Graduate School of Medicine, Kobe 650-0017, Japan; §Infectious and Inflammatory Diseases Center, Sanford-Burnham Medical Research Institute, La Jolla, CA 92037; and ¶Department of Integrative Medical Biology, Section for Histology and Cell Biology, Umeå University, SE-901 87 Umeå, Sweden

Received for publication February 18, 2011. Accepted for publication May 4, 2011.

This work was supported by a Grant-in-Aid for Scientific Research on Priority Areas Cancer, a Grant-in-Aid for Scientific Research (B), a Grant-in-Aid for Young Scientists (B), a grant of the Global Center of Excellence Program from the Ministry of Education, Culture, Sports, Science, and Technology of Japan, and Grants R37AI33068, AI067890, and AI088445 from the U.S. National Institutes of Health (to C.F.W.).

Address correspondence and reprint request to Prof. Takashi Matozaki, Division of Molecular and Cellular Signaling, Department of Biochemistry and Molecular Biology, Kobe University Graduate School of Medicine, 7-5-1 Kusunoki-cho, Chuo-ku, Kobe 650-0017, Japan. E-mail address: matozaki@med.kobe-u.ac.jp

The online version of this article contains supplemental material.

Abbreviations used in this article: BM, bone marrow; cDC, conventional dendritic cell; DC, dendritic cell; FRC, fibroblastic reticular cell; KO, knockout; LIGHT, lymphotoxin-like, exhibits inducible expression and competes with HSV glycoprotein D for herpes virus entry mediator, a receptor expressed by T lymphocytes; LN, lymph node; LT, lymphotoxin; LTi, lymphoid tissue inducer; LTβR, lymphotoxin β receptor; MT, mutant; PALS, periarterial lymphoid sheath; pLN, peripheral lymph node; SHP, Src homology 2 domain-containing protein tyrosine phosphatase; SIRPα, signal regulatory protein α; WT, wild-type.

www.jimmunol.org/cgi/doi/10.4049/jimmunol.1100528

matrix proteins. SIRPα is especially abundant in DCs or macrophages, whereas it is barely detectable in T or B lymphocytes (13–17). The extracellular region of SIRPα interacts with the ligand CD47, which is also a member of the Ig superfamily (12, 13, 18). In contrast to the relatively restricted distribution of SIRPα, CD47 is expressed in most cell types including a variety of hematopoietic cells (18).

SIRPα and CD47 constitute a cell–cell communication system, and such interaction plays important roles in both hematopoietic and immunological regulation. The interaction of CD47 on hematopoietic cells to SIRPα on macrophages is thought to prevent phagocytosis through an SIRPα-dependent activation of SHP-1 (13, 15, 19, 20). The SIRPα activation of SHP-1 determines both the life span of individual RBCs and the number of these cells in the circulation (13, 15, 19, 20). The SIRPα–CD47 interaction is also implicated in prevention of the clearance by splenic macrophages of transfused platelets or lymphocytes from the bloodstream (21–23), as well as in regulation of the ability of macrophages to discriminate between viable and apoptotic cells (24). Moreover, the interaction of SIRPα in DCs with CD47 expressed in either hematopoietic or nonhematopoietic cells (such as stromal cells) is also important for homeostasis of conventional DCs (cDCs), particularly $CD8^-$ cDCs in secondary lymphoid organs through the regulation of the survival of cDCs (25–27).

Although the expression of SIRPα is minimal in T or B cells in the mouse spleen (as shown in Supplemental Fig. 1), we show that the size of T cell zone, as well as the number of $CD4^+$ T cells in the spleen are markedly decreased in mice bearing a mutant (MT) version of SIRPα or CD47-deficient (CD47 knockout [KO]) mice. SIRPα and CD47 are thus important for the homeostasis of T cells in the spleen.

Materials and Methods

Abs and reagents

An agonistic rat mAb to mouse LTβR (4H8) was described previously (28, 29). A rat mAb to mouse CD16/32 (2.4G2) was isolated from the culture supernatant of hybridoma cells (kindly provided by K. Okumura, Juntendo University, Tokyo, Japan). A rat mAb to mouse SIRPα (kindly provided by C.F. Lagenaur, University of Pittsburgh, Pittsburgh, PA) was purified from culture supernatants of hybridoma cells. The mAbs were conjugated to sulfo-NHS-LC biotin [sulfosuccinimidyl-6-(biotinamido) hexanoate; Pierce]. Goat anti-mouse CCL21, CCL19, and CXCL13 polyclonal Abs were purchased from R&D Systems. Cy3-conjugated donkey Abs to goat IgG and hamster IgG were from Jackson ImmunoResearch Laboratories. FITC-conjugated mAbs to mouse B220 (RA3-6B2) and CD4 (L3T4), biotin-conjugated mAbs to mouse Thy1.2 (30-H12) and CD19 (eBio1D3), and a hamster mAb to mouse gp38 (ebio8.1.1) were from eBioscience. FITC-conjugated mAbs to CD8α (53-6.7), an allophycocyanin-conjugated mAb to CD11c, biotin-conjugated mAbs to CD4 (RM4-5), and FITC- or PE-conjugated streptavidin were obtained from BD Biosciences. Allophycocyanin-Cy7–conjugated mAb to B220 (RA3-6B2) were from BioLegend (San Diego, CA). Anti-biotin microbeads were from Miltenyi Biotec (Bergisch Gladbach, Germany). RPMI 1640 medium (Sigma-Aldrich) was supplemented with 10% heat-inactivated FBS, 50 μM 2-ME, 2 mM L-glutamine, 10 mM HEPES-NaOH (pH 7.4), penicillin (100 U/ml), streptomycin (100 μg/ml), and 1 mM sodium pyruvate to yield complete medium.

Animals

Mice that express an MT version of SIRPα lacking most of the cytoplasmic region were described previously (30, 31). The mice were backcrossed onto the C57BL/6 background for five generations. CD47 KO mice were described previously (19, 25) and backcrossed to the C57BL/6 background for >10 generations. Sex- and age-matched mice at 6–12 wk of age were studied. Mice were bred and maintained in the Institute of Experimental Animal Research of Gunma University under specific pathogen-free conditions, and care and use were in accordance with the animal care guidelines of Gunma University.

Histological and immunohistofluorescence analyses of the spleen or peripheral LNs

For histological analysis, the spleen or peripheral LNs (pLNs) were removed and immediately fixed with 4% paraformaldehyde in 0.1 M sodium phosphate buffer (pH 7.4). Paraffin-embedded sections (4 μm) were stained with Mayer's H&E. For immunohistofluorescence analysis, the spleens were directly embedded in optimal cutting temperature compound (Sakura) and immediately frozen in liquid nitrogen, followed by cutting into 8-μm sections and fixation in 4% paraformaldehyde in 0.1 M phosphate buffer. All sections were incubated for 1 h at room temperature in blocking solution (PBS with 5% BSA) and then stained with primary Abs diluted in PBS containing 5% BSA and 0.3% Triton X-100 overnight at 4°C. They were then washed with PBS, stained with Cy3- or FITC-conjugated Abs diluted in PBS containing 1% BSA and 0.3% Triton X-100 for 1 h at room temperature, and they were washed again with PBS. Fluorescence or bright-field images were acquired with a BX-51 microscope (Olympus), a color cooled CCD camera (DP71; Olympus), and DP controller software (Olympus). For measurement of areas for the T zone and B zone or of gp38-positive regions in the spleen, cross-sections were made through central segments of the spleen, stained for Thy1.2 and B220 or gp38, and images were then acquired at ×4 (T zone and B zone) or ×10 (gp38) objective magnification, respectively. By the use of Image J software (National Institutes of Health), the values for positively stained regions in a microscopic image of the spleen from each mouse were obtained and averaged.

Cell preparation and flow cytometry

Cell suspensions were prepared from spleen or pLNs as described previously (25). For preparation of splenocytes or pLN cells, the spleen or pLNs were minced and then digested with collagenase (Wako) at 400 U/ml in the presence of 5 mM EDTA for 30 min at 37°C. The undigested fibrous material was removed by filtration through a 70-μm cell strainer (BD Falcon), and RBCs in the filtrate were lysed with Gey's solution. The remaining cells were washed twice with PBS and then subjected to flow cytometric analysis. The cells were first incubated with an mAb to mouse CD16/32 to prevent nonspecific binding of labeled mAbs to Fcγ receptors and then stained with a biotin-conjugated mAb to mouse CD4. The cells were washed and incubated with an FITC-conjugated mAb to mouse CD8, PE-conjugated streptavidin, allophycocyanin-conjugated mAb to CD11c, and allophycocyanin-Cy7–conjugated mAb to B220. The cells were washed again before suspension in the presence of propidium iodide to identify dead cells and analyzed by flow cytometry with the use of an FACSCanto II or FACSAria II instrument (BD Biosciences) and FlowJo software (Tree Star).

Preparation of cDNA and quantitative real-time PCR

Total RNA was extracted from the freshly isolated spleen using Qiazol and the RNeasy mini kit (Qiagen) according to the manufacturer's instructions. The first-strand cDNA was synthesized from 1 μg total RNA using the QuantiTect Reverse Transcription kit (Qiagen) according to the manufacturer's instructions. cDNA fragments of interest were amplified using the QuantiTect SYBR Green PCR kit (Qiagen) on LightCycler 480 (Roche Applied Science) in 96-well plates (Roche Diagnostics). The amplification results were analyzed by the use of LightCycler 480 software (Roche Applied Science) and then normalized with GAPDH levels for each sample. Primer sequences for quantitative real-time PCR were as follows: *Ccl21*, forward: 5′-ATCCCGGCAATCCTGTTCTC-3′, reverse: 5′-GGGGCTTTGTTTCCCTGGG-3′; *Ccl19*, forward: 5′-GGGGTGCTAATGATGCGGAA-3′, reverse: 5′-CCTTAGTGTGGTGAACACAACA-3′; *Cxcl13*, forward: 5′-GGCCACGGTATTCTGGAAGC-3′, reverse: 5′-GGGCGTAACTTGAATCCGATCTA-3′; *Lta*, forward: 5′-TCCACTCCCTCAGAAGCACT-3′, reverse: 5′-AGAGAAGCCATGTCGGAGAA-3′; *Ltb*, forward: 5′-TGCGGATTCTACACCAGATCC-3′, reverse: 5′-ACTCATCCAAGCGCCTATGA-3′: *Tnfsf14* (LT-like, exhibits inducible expression and competes with HSV glycoprotein D for herpes virus entry mediator, a receptor expressed by T lymphocytes [LIGHT]), forward: 5′-CAACCCAGCAGCACATCTTA-3′, reverse: 5′-ATACGTCAAGCCCCTCAAGA-3′; *LtbR*, forward: 5′-AGCCGAGGTCACAGATGAAAT-3′, reverse: 5′-CCCTGGATCTCACATCTGGT-3′; *Il7*, forward: 5′-GATAGTAATTGCCCGAATAATGAACCA-3′, reverse: 5′-GTTTGTGTGCCTTGTGATACTGTTAG-3′; *Nfkb2* (p100), forward: 5′-CTGCTGCTAAATGCTGCTCA-3′, reverse: 5′-AGCAGTTGCTCCAGGTTCTG-3′; and *Gapdh*, forward: 5′-AGGTCGGTGTGAACGGATTTG-3′, reverse: 5′-TGTAGACCATGTAGTTGAGGTCA-3′.

Bone marrow chimeras

Recipient wild-type (WT) or MT mice were subjected to lethal irradiation (9.5 Gy) and then injected i.v. with 5×10^6 bone marrow (BM) cells obtained from either WT or MT donor mice as described previously (25). Six to 8 wk after BM transplantation, the recipient mice were killed, and the spleen was subjected for histology, immunohistofluorescence analysis, and extraction of RNA for real-time PCR.

Isolation of T and B cells

The spleen was gently ground with sterilized frosted slide glasses in PBS followed by filtration through a 70-μm cell strainer (BD falcon) to remove fibrous components. RBCs were lysed with Gey's solution and washed twice in PBS. For isolation of T cells, splenocyte suspension was filtrated again through nylon wool before purification. T or B cells were purified with the use of magnetic beads coated with a biotin-conjugated mAb to Thy1.2 or CD19, respectively, and an MACS column (Miltenyi Biotec). The purity of the isolated Thy1.2$^+$ T cells or CD19$^+$ B cells were >90% as determined by flow cytometry.

Analysis of in vivo gene expression by the injection of agonistic mAbs to LTβR

In vivo injection of agonistic mAb to LTβR was performed as described previously with minor modifications (28). In brief, WT or MT mice were injected i.p. either with 50 μg control rat IgG Ab or 50 μg agonistic anti-LTβR mAbs. Twenty-four hours later, spleen was isolated and cDNA was prepared, and then mRNA expression of CCL21 (*Ccl21*) or NFκb2 p100 (*Nfkb2*) was analyzed by real-time PCR.

Statistical analysis

Data are presented as means ± SE and were analyzed by Student *t* test or by one-way ANOVA, and post hoc comparisons were made using the Tukey-Kramer test with use of Stat View 5.0 software (SAS Institute). A p value <0.05 was considered statistically significant.

Results

Impairment of T cell zone development in the spleen of SIRPα MT mice

We previously showed that the SIRPα MT mice displayed mild splenomegaly characterized by expansion of the red pulp (15) (Fig. 1*A*). The expanded red pulp of the spleen was attributable to an increase in erythropoiesis to compensate for persistent anemia caused by increased phagocytic clearance of RBCs. The MT SIRPα protein expressed in the transgenic mice fails to undergo tyrosine phosphorylation or form a complex with SHP-1 or SHP-2 (20). Given the importance of the cytoplasmic region of SIRPα for signaling by this protein, the function of SIRPα is thought to be eliminated in the MT mice (15, 20). In contrast to the expanded red pulp, the white pulp in SIRPα MT mice was significantly smaller and more segmented when compared with WT mice (Fig. 1*A*). Quantitative immunohistofluorescence analyses of T cells (Thy1.2$^+$) and B cells (B220$^+$) in the spleens of SIRPα MT mice revealed the area of the white pulp was markedly reduced, particularly in the T cell zone around the arteriole (Fig. 1*B*, 1*C*). We consistently observed that the number of CD4$^+$ T cells in the spleen of SIRPα MT mice was markedly decreased compared with that of WT mice (Fig. 1*D*). The number of CD8$^+$ T cells was slightly decreased in the spleen of SIRPα MT mice, although such decrease was not statistically significant. By contrast, the number of B cells in the spleen did not differ between WT and SIRPα MT mice (Fig. 1*D*). The size of T cell zones as well as the absolute number of CD4$^+$ or CD8$^+$ T cells in pLNs did not differ between WT and SIRPα MT mice (Supplemental Fig. 2). The proportions of CD4$^+$ T cells as well as CD8$^+$ T cells and B cells in the peripheral blood of MT mice were also similar to those apparent for WT mice (Supplemental Fig. 3). These results suggest that the alteration of the T cell zone is specific to the spleen of SIRPα MT mice.

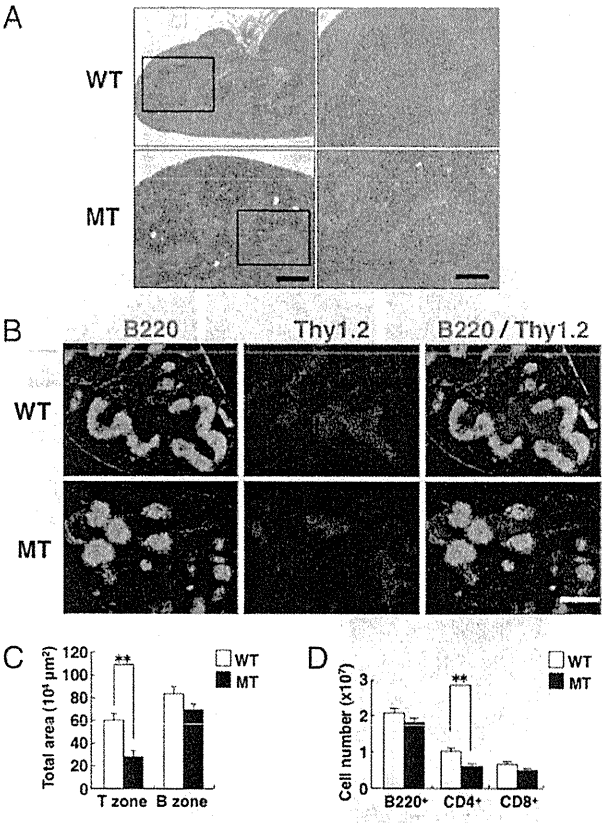

FIGURE 1. Impairment of T cell zone development in the spleen of SIRPα MT mice. *A*, Paraffin sections of the spleen from WT or SIRPα MT mice were stained with H&E. The boxed regions of the *left panels* are shown at higher magnification in the *right panels*. Scale bars, 500 μm (*left panels*) and 200 μm (*right panels*). *B*, Frozen sections of the spleen from WT or MT mice were double-stained with an mAb to B220 (green) and an mAb to Thy1.2 (red). Scale bar, 500 μm. *C*, By the use of Image J software (National Institutes of Health), the areas for Thy1.2-positive T cell zones or B220-positive B cell zones in the spleen sections prepared as in *B* was measured per each image. Data are means ± SE for a total of five mice per group in three independent experiments. *D*, The absolute numbers of B cells (B220$^+$), CD4$^+$ T cells (CD4$^+$), and CD8$^+$ T cells (CD8$^+$) in the spleen of WT or MT mice were determined by flow cytometry. Data are means ± SE for four mice per group and representative of three independent experiments. $^{**}p < 0.01$ (Student *t* test).

Reduced expression of CCL-19, CCL-21, and IL-7 in the spleen of SIRPα MT mice

The smaller size of the T cell zone as well as the reduced number of CD4$^+$ T cells in the spleen of SIRPα MT mice suggested that homing or survival of T cells is impaired in the MT mice. Expression levels of CCL19, CCL21, and CXCL13 mRNA in the spleen of SIRPα MT mice were markedly decreased in MT mice compared with WT mice (Fig. 2*A*). Immunohistofluorescence analysis showed a loss of CCL19 and CCL21 in the T cell zone of SIRPα MT mice, whereas CXCL13 in the B cell follicles appeared the same as in WT mice (Fig. 2*C*). IL-7 is important for the survival and homeostasis of T cells (6). We found that IL-7 mRNA expression in the spleen of SIRPα MT mice was also markedly decreased compared with that of WT mice (Fig. 2*B*). Thus, both recruitment and survival of T cell may be compromised in SIRPα MT mice. FRCs in the T cell zone express CCL19, CCL21, and IL-7 (1, 6), suggesting a defect in the stromal cells in SIRPα MT mice. The expression of the mucin gp38, which identifies FRCs in the T cell zone (32, 33), was